Glial Clusters and Psychopathology: Exploring Reduced Counts With a Person's Diagnosis of Schizophrenia or Bipolar Disorder and Finding Novel Cluster Morphology

Glial Clusters and Psychopathology: Exploring Reduced Counts with a Person's Diagnosis of Schizophrenia or Bipolar Disorder and Finding Novel Cluster Morphology

Arthur Theodore Grayson III

A Thesis in the Field of Psychology

for the Degree of Master of Liberal Arts in Extension Studies

Harvard University

November 2018

Abstract

Schizophrenia (SZ) and Bipolar Disorder (BD) are both severe psychiatric disorders that permanently alter a person's life by afflicting their cognitive and emotional faculties. Over the course of a person's life, the symptoms might vary in severity, but the changes in neurological determinants of their cognitive and emotional function keep a biological score. Deficits in functional connectivity unique to the two disorders have been associated with alterations in the extracellular matrix (ECM), a loose chemical substance that acts as a chemical medium for cells to communicate and build structural and functional networks, as well as performing a host of other functions. Aside from the ECM itself being a structure found throughout the brain, various tightly organized aggregates of the ECM have been studied due to their potential role in regulating neuronal activity, which then has downstream effects on cognitive and emotional function. Previous investigations from the authors' lab have found novel ECM structures called 6-sulfated chondroitin (CS-6) glial clusters, which consist of 6-sulfated structures associated with glial cells. Findings from these investigations indicate glial clusters may be involved in synaptic regulation. Researchers from the lab have previously reported marked reductions of these clusters in the amygdalae of persons diagnosed with SZ or BD compared to healthy people. Informed by these findings, these authors theorized that glial clusters may be involved in the cognitive and emotional processing deficits suffered by people with psychotic disorders, and sought to extend findings from the amygdala to the mediodorsal thalamic nucleus (MDTN) to find quantifiable evidence to support this theory. The

MDTN was chosen due to its numerous, reciprocal axonal connections with the prefrontal cortex, where imaging studies have shown marked reductions in functional activity and connectivity in persons with SZ and BD. Authors hypothesized cluster counts would be decreased in the MDTN of persons with either a psychiatric diagnosis of SZ or BD compared to controls. Quantification of CS56 immunoreactive clusters in the MDTN showed significant reductions for total number in persons with a diagnosis of SZ or BD compared to control, and for numerical density as well, with no change in volume of the nucleus between groups. During the current investigation, high resolution microscopic imaging of the clusters stained by immunoreaction to CS56 (a CS-6 specific antibody) also led investigators to find distinctions in morphology, indicating heterogeneity not previously seen. Authors detail their classification system, which revealed four novel morphological cluster types: a *tendril type*, a *diffuse type*, a *densely diffuse type*, and a fourth type called *type-4*. Discovery of morphological characteristics for clusters provides new avenues for researching neuropathological development in psychotic disorders, and findings of cluster reductions indicates a potential role for this ECM structure in the network disruptions resulting in cognitive and emotional deficits for persons with SZ and BD.

HARVARD UNIVERSITY

MASTERS OF LIBERAL ARTS IN EXTENSION STUDIES

CONCENTRATION: PSYCHOLOGY

GLIAL CLUSTERS AND PSYCHOPATHOLOGY: EXPLORING REDUCED COUNTS WITH A PERSON'S DIAGNOSIS OF SCHIZOPHRENIA OR BIPOLAR DISORDER AND FINDING NOVEL CLUSTER MORPHOLOGY

Thesis Director:

Associate Professor Sabina Berretta, M.D.

Thesis Advisor:

Dante Spetter, Ph.D.

Master's Thesis of:

Arthur Theodore Grayson III

Academic Year 2017 – 2018

Biography & Dedication

I am the son of two loving people, whose not-too-distant ancestors were slaves, whose ancestors before them are unknown to us now, and were unwillingly brought to this country, foisted into torturous work and insufferable living conditions, had dehumanizing identities foisted upon them, and were made to believe their lineage would fare no better than they. Now, the son of two proud Black American parents graduates from Harvard University. I am lucky to have lived long enough to continue to pay them back for all the years they invested in me, backed me against incredible odds, tolerated my whims, and watched anxiously or hopefully as I went after what I wanted. I am deeply honored to say that this will not be the pinnacle of accomplishment with which I am able to bless my parents. What a day, that I can deny such a grand institution the status of "my greatest achievement" as a Black man in America! Yes, my son, my daughter, niece, nephew, or kinfolk, there are grander things beyond these hallowed ivory walls, and numerous means by which to achieve them. One day, this monumental milestone can, for us, be as commonplace as a humble high-school diploma. I envisage a great and bountiful future ahead of our family, that perhaps you, dear reader, are already taking part in. Here, I lay my brick in the path being built toward that future, and dedicate this monumental thesis to my parents, Arthur & Michelle Grayson, who paved the way for my brick-laying with theirs; and to my sister, Clarissa, for sharpening my iron with hers all these years; my sister Jeanée and her family; my brother, Michael; my Aunt Pudgy; my brother, Aaron; and to all our extended family. Who's got next?

Acknowledgments

In an expression of deep gratitude, I thank my thesis director, Dr. Sabina Berretta for creating such a welcoming laboratory in which many a great mind has come and become better scientists, now including myself. Thank you for your time, your trust, encouragement, and incisive guidance you've shared with me unsparingly over these past two years. I also thank Dr. Harry Pantazopoulos for being so positive and helpful with training, all the continuous learning of so much more neurobiology than I ever hoped to need, and for keeping the lab a cool, Superhero-Friday space! Thank you for mentoring me above all else throughout this program, Harry, and for honestly believing in what I set out to accomplish; that made it easier for me to ask for reasonable advice and to have reasonable expectations for my work, without which I would have missed so many deadlines. I thank all of my labmates at TNL with whom I trained and shared in the woes and throes of thesis life, and wish you all the smoothest transitions into your next phases of life and happiness. To all of my great friends in Cambridge and beyond who saw me through this journey and rooted me on, read drafts of the proposal and this thesis, and had beers or dinners or long conversations with me about the lives we had been leading during this time, its meaning, and getting through it all, I love you and thank you: Anovators (Sunder and Lauren), and extended Anovatorians (Laura, Ikram, Kimmy, and Gautham), Yvette and Dexter, Charles and Shardae, Reed, Carlos, Jonathan, Jonah, Josh and Tony, Ali, and Matthias. Finally, big ups to the Harvard Black Graduate Student Alliance (HBGSA), which came into my life just in the nick of time!

Table of Contents

List of Tables

List of Figures

Chapter I

Introduction

Schizophrenia and bipolar disorder are among the most severe psychiatric disorders. They each have prominent but differing hallmark presentations, but also share some overlapping cognitive pathologies. Overlapping deficits between both disorders that can be tested in neuropsychological assessments include attention, working memory, executive function, disorganized thinking, and emotional dysfunction (Amann et al., 2012; Andreasen, Paradiso & O'Leary, 1998; Harrison, 2016; Yu, Cheung, Leung, Li, Chua, & McAlonan, 2010). Imaging studies run while testing these same attributes confirm decreased activation and connectivity in the prefrontal cortex for both disorders (Argyelan et al., 2009; Jang & Yeo, 2014; Lewis & Sweet, 2009). Clinical and neuroimaging studies have enumerated the symptoms, but neither are able to explain the psychological differences between healthy individuals and those suffering from schizophrenia (SZ) or bipolar disorder (BD).

Authors of the present investigation sought to investigate whether neuropathology (brain abnormality) could account for the overlapping symptomology and functional deficits in SZ and BD compared to unaffected individuals. A postmortem investigation—examining donated brain tissue from deceased donors—offered the best chance for a clue to better connect the knowledge base of functional activation findings with clinical case studies. Following a brief overview of the two brain disorders, this chapter will cover the rationale for a postmortem investigation, review prior postmortem evidence, detail the

researchers' region of interest for this investigation, and finally, conclude with remarks on the relevance of the current study to broader empirical findings.

Living with Psychiatric Illness

SZ is a developmental brain disorder with often devastating effects on the family of a diagnosed member, and drastic lifestyle limitations for the affected individual (Lewis & Leiberman, 2000 & Lewis & Sweet, 2009). Relatively low in prevalence, most estimates of lifetime risk show SZ afflicts one in every hundred people worldwide (Aleman & Kahn, 2005; Lewis et al., 2009; Lindenmayer, Harvey, Khan, & Kirkpatrick, 2007). There is a higher incidence of the disorder in men than women (Aleman et al., 2005 & Lewis et al., 2009) by a ratio of about 1.4:1 (McGrath, Saha, Chant, & Welham, 2008). People with SZ can present with a broad array of positive symptoms (pathological behaviors clinically present that are usually not) and negative symptoms (otherwise normal behaviors that should be present, but pathologically are not) (Aleman et al., 2005; Lewis et al., 2000 & 2009; MacDonald & Schultz, 2009; Peralta & Cuesta, 2001). Distinct symptomatology and functional deficits are consistently documented in the symptomology of SZ. These can include deficits in reasoning, memory, attention and perception (Aleman et al., 2005), as well as dysmetria (Andreasen, Paradiso & O'Leary, 1998), and sensory gating (Van der Werf, Jolles, Witter, & Ulyings, 2003). These functional deficits in people with SZ measured by neuropsychological assessments are of most relevance to the present investigation as they heavily recruit the use of the frontal cortex.

BD is a mood disorder marked by distinctly cyclical states of affective dysfunction. People with this disorder experience periods of depression, emotional dysfunction (swinging from mania to euthymia with mixed mood states), social withdrawal, and psychosis (Harrison, 2016). People suffering the disorder commit suicide at a rate of 5% (Harrison, 2016), and there is a lifetime prevalence of BD in the US population of 3.3% with no gender differences (Grant et al., 2005). BD is one of the most highly heritable psychoses based on studies for genetic concordance among identical twins with findings between 50% to 80% (Harrison, 2016). This thesis emphasizes the overlap between these two forms of severe psychopathology, the common functional deficits, psychosis and perceptual aberrations, and the neuropathology potentially underpinning them all in both conditions (Amann et al., 2012; Argyelan et al., 2014; Kahn, 2012; Yu, Cheung, Leung, Li, Chua, & McAlonan, 2010). Functional deficits documented in both disorder populations include memory impairments, lowered frontal activation on fMRI called hypofrontality, executive dysfunction, perceptual deficits and more (Argyelan et al., 2014; Chai et al., 2011; Martinot et al., 1990; Pergola, Selvaggi, Trizio, Bertolino, & Blasi, 2015).

Rationale for a Postmortem Study of SZ & BD

Given these overlapping symptoms, researchers have tried to identify common underlying neurological and neuroanatomical abnormalities. In both disorders, evidence suggests a disruption in connectivity between the thalamus and prefrontal cortex. Because the thalamus is responsible for reciprocal information to and from the cortex for sensory processing, this dysconnectivity may help explain the deficits common to SZ and BD

(Anticevic et al., 2010; Woodward, Karbasforoushan, & Heckers, 2012; Pergola et al., 2015; Welsh, Chen & Taylor, 2010). The disruption of thalamocortical pathways has been documented in studies employing functional magnetic resonance imaging (fMRI) (Marenco et al., 2012).

Imaging studies have shown that emotional and cognitive deficits are related to lowered levels of fMRI activation in cortical regions connected with the amygdala and thalamus in both SZ and BD (Aleman & Kahn, 2005; Chai et al., 2011; Soares & Mann, 1997; Welsh, Chen & Taylor, 2010). Some imaging studies have found changes in brain pathway connectivity associated with these two disorders. Anticevic et al. (2013) replicated the finding that both higher and lower connectivity in the brain is associated with SZ and BD using blood oxygenation level-dependent (BOLD) signal during resting-state functional connectivity magnetic resonance imaging (fcMRI). They found associations for increased connectivity between bilateral sensory and motor cortices, as well as decreased connectivity between the prefrontal cortex, cerebellum and thalamus in both populations (Anticevic et al., 2013). Despite a robust sample, they were unable to identify the specific altered pathway most reliably associated with diagnosis. In 2015, using whole brain resting-state imaging approach with over 400 diagnosed individuals and over 400 healthy controls, Cheng et al. (2015) were able to show the greatest network changes between diagnosed individuals and healthy controls. Their data showed the most significant increased connectivity among people diagnosed with SZ or BD was the pathway between the thalamus and primary somatosensory cortex, but a decreased network connectivity was found most significantly between the thalamus and frontal cortex (Cheng et al., 2015). These results allowed Cheng et al. to suggest changes in

networks as potentially a reliable diagnostic indication for differentiating people with SZ or BD from neurotypical individuals. An over-connected thalamus to primary motor and sensory cortex and an under-connected thalamocortical pathway potentially explains overlapping symptoms of SZ and BD such as sensory gating and psychosis (Anticevic et al., 2013; Javitt & Freeman, 2015; Woodward, 2012). Other research teams have seen volumetric decreases of both the amygdala and thalamus in diagnosed people compared to people without either diagnosis (Byne et al., 2002 & Dorph-Peterson et al., 2004). Studies that began to find brain changes in the thalamus associated with hypofrontality have lead to the theory of thalamocortical dysconnectivity—that a disruption in the pathway between the thalamus and frontal cortex could account for symptoms of SZ and BD (Marinot et al., 1990). Where imaging studies fall short, however, is in a lack of molecular resolution for a more fine-grained analysis of the brain structures most associable to diagnosis and even symptom severity. A postmortem study investigating structural changes at the cellular level is needed for this, and could offer a unifying explanation for thalamocortical dysconnectivity, volumetric decreases, neuronal count decreases, and ECM abnormalities for both SZ and BD populations.

Prior Postmortem Evidence

Postmortem histological research is beginning to support fMRI findings. Over a dozen postmortem studies have shown findings of reduced volume, density, and neuronal and glial cell count in the thalamus of people with psychotic disorders (Anticevic et al., 2015; Danos et al., 2003; Dorph-Petersen & Lewis, 2017; Pakkenberg, 1990; Popken, Bunney, Potkin, & Jones, 2000; Van der Werf, 2003; Young, Manaye, Liang, Hicks, &

German, 2000). This neuropathology could explain the disruption of signals from the thalamus to the frontal cortex. In this specific instance of pathway disruption, postmortem investigations have shown great potential to further illuminate how thalamic cytoarchitecture contributes to the pathogenesis of frontal activity deficits as was noted in a review by Pergola et al. in 2015. Popken et al. (2000) conducted an empirical postmortem investigation linking subnucleus cell loss to diagnosis with the most closely matched pathological–control study published to date. Despite their small cohort size, 6 diagnosed people and 6 control people, their data detected large differences. Popken et al. found the subnucleus within the mediodorsal thalamic nucleus most densely connected with the prefrontal cortex in control individuals, the parvocellular subnucleus, had the largest decrease in cell count for tissue samples from donors diagnosed with SZ compared to controls (2000). Knowing how cell morphology relates to disrupted pathways associable to diagnosis is an important step toward making correlation-based inferences about etiology or reliable assumptions for diagnosis. Apoptosis, lower cell densities, demyelination, and loss of glial support could be the cause for reduced connectivity and reduced activity.

The Extracellular Matrix & Clusters

The brain is made of three main materials: neurons, glia and extracellular matrix (ECM). Neuronal bodies, or soma, make up the grey matter, while axonal projections from soma outward make up the white matter tracts. Glial cells can be found in both grey and white matter. The interstitial space between them is the ECM. It is comprised of a loose chemical substance that pervades the cortices, subcortical structures, even synapses,

and of which accounts for roughly 20% of the brain's volumetric mass (Berretta, 2012; Sykova & Nicholson, 2008). Chondroitin sulfate proteoglycans are a major molecular component of the ECM (Berretta, 2012). They have been found to form richly organized structures surrounding certain neuronal and glial cells in the brain as perineuronal nets, forming into arrangements of ECM aggregates throughout the intersynaptic domain as clusters, as well as around and along axons as axonal coats (Berretta, 2012; Pantazopoulos et al., 2015a; Pantazopoulos, Turiak, King, Zaia, & Berretta, 2015b). When preferentially surrounding the soma and dendritic arbors of single neurons, these molecules of the matrix are called perineuronal nets (PNNs) (Berretta et al., 2015). PNNs confer several properties to neurons including facilitating neurodevelopment (neuronal migration, axon outgrowth and closure of critical periods of neurodevelopment), cell differentiation, stabilization of neuronal plasticity, and regulation of receptor trafficking. They are also believed to protect certain classes of neurons against oxidative stress (Berretta, 2012; Miyata, Komatsu, Yoshimura, Taya, & Kitagawa, 2012; Pantazopoulos et al., 2010 & 2015a). Importantly, PNNs mature during critical periods of neurodevelopment in the late adolescent period, which aligns with the typical age of onset of SZ (Berretta, Pantazopoulos, Markota, Brown, & Batzianouli, 2015a).

The quadripartite synapse—or the junction created by the axon terminal, post-synaptic site, involved glial processes, and the ECM pervading it all (Pantazopoulos & Berretta, 2015)—is a fresh concept as the functional unit wherein neurotransmission occurs. Large macromolecules of the ECM, chondroitin sulfate proteoglycans, form aggregates of 6-sulfated chondroitin chains, expressed around the bundled processes of glia and throughout the intersynaptic domain (Hayashi et al., 2007; Miyata et al., 2012;

Pantazopoulos et al., 2015a). These aggregates can be stained and identified with a histological antibody called CS56. These stained aggregates, called "glial clusters," are under investigation. ECM clusters, hereafter referred to as CS56-immunoractive (CS56-IR) clusters or simply clusters, could provide the same protection and facilitation for synaptic stability and plasticity for multiple neurons as PNNs do for single neurons. However, research has not yet determined what function CS56-IR clusters serve (Hayashi et al., 2007; Miyata et al., 2012; Pantazopoulos et al., 2015a). Further support for investigating cluster counts in the thalamus comes from a study on axonal coats. The same chondroitin sulfate proteoglycans forming PNNs and CS56-IR clusters, also form around the axons of single neurons as axon coats (Pantazopoulos et al., 2015b). Pantazopoulos et al. (2015b) found differences in axonal coat counts associated with diagnosis in the mediodorsal thalamic nucleus of people with SZ, potentially contributing to thalamocortical dysconnectivity. Likewise, PNNs ensheathing certain classes of neurons are markedly decreased in the amygdalae of people with SZ, potentially contributing to the observed emotional processing deficits due to dysfunction of inhibitory networks (Berretta et al., 2015 & Pantazopoulos et al., 2015a). To see if a reduction in the numbers of clusters in the intersynaptic domain are likewise associated with symptoms and functional deficits as is postulated with PNNs and axonal coats, a closer evaluation into their potential role in thalamocortical dysconnectivity is needed.

The MDTN as the Region of Interest

The mediodorsal thalamic nucleus (MDTN) sits on the top and middle-most side of the thalamic lobes. Neurons here project heavily myelinated axons to association

cortices in the prefrontal area, and also receive projections from the same. The association cortex in this area handles cognitive associations as compared to primary sensory cortices such as M1, S1, V1, etc. (Jang & Yeo, 2014 & Dorph-Petersen, 2017). These reciprocal pathways between the prefrontal cortex and the MDTN are disrupted, resulting in lowered connectivity and activation in functional imaging studies in people diagnosed with SZ and BD (Andreasen et al., 1998; Anticevic et al., 2013; Danos et al., 2003; Dorph-Petersen & Lewis, 2017; Martinot et al., 1990; Pakkenberg, 1990; Popken et al., 2000; Van der Werf, 2003; Young, Manaye, Liang, Hicks, & German, 2000). The mediodorsal is one of the most studied thalamic nuclei with postmortem techniques for SZ research (Dorph-Petersen & Lewis, 2017 & Popken et al., 2000). It is known to contribute to aspects of memory, specifically executive function, attention, and other complex cognitive functions (Dorph-Petersen & Lewis, 2017 & Popken et al., 2000). A reduction in thalamic connectivity to the prefrontal cortex (Anticevic et al., 2010; Marenco et al., 2012; Pergola et al., 2015; Welsh et al., 2010; Woodward et al., 2012), as well as reductions in neuronal count and volume in the MDTN of people with SZ (Andreasen et al., 1998; Danos et al., 2003; Dorph-Petersen & Lewis, 2017; Pakkenberg, 1990; Young, Manaye, Liang, Hicks, & German, 2000) suggest the neuropathology associated with perceptual symptoms and functional deficits of psychosis. But early indications of these pathway disruptions originally came from cortical lesions in clinical cases. For example, in one such case of a person with a lacunar infarction directly next to the MDTN, Van der Werf et al. (1999) showed that a lesion at one end of the thalamocortical pathway (in the thalamus) yields the same functional deficits as a lesion on the other end (in the cortex).

The MDTN is comprised of further subnuclei that can be identified by the groupings and projections of their neurons, those being the magnocellular, parvocellular & densocellular nuclei (Popken et al., 2000). Among the three subnuclei, the parvocellular had the greatest reduction in total number of neurons, showing 30.9% fewer for people with SZ compared to healthy controls (Popken et al., 2000). Heavily myelinated axonal projections from the parvocellular directly connect to the dorsolateral prefrontal cortex (DLPFC) (Popken et al., 2000). The DLPFC is the same area in the frontal lobe known for thalamocortical disruptions in BD.

Hypofrontality in BD (Martinot et al., 1990) has direct relevance to thalamocortical dysconnectivity (Anticevic et al., 2015). Well-established disturbances in top-down processing such as deficits in DLPFC activation in BD during tasks of attention and working memory as well as executive function are potentially indicative of disrupted connectivity (Martinot et al., 1990; Marvel & Paradiso, 2004; Soares & Mann, 1997). Postmortem studies show reductions in the numbers of neuron and glia in the DLPFC of people with BD (Ongür, Drevets & Price, 1998 & Rajkowska, Halaris & Selemon, 2001). It seems straightforward to infer a link between reduced grey matter in the frontal cortices and disrupted thalamocortical activation, but a recent study found that reduced cortical thickness alone does not account for it (Skåtun et al., 2017). The authors concluded the thalamus is the more important target of investigations in deciphering the dysconnectivity across brain disorders. Neuropathological correlates to disruptions in higher cognitive function must now be drawn by postmortem investigations into the pathway from the thalamus to the DLPFC.

Very recent discoveries in the amygdala of people with SZ and BD, the findings surrounding the potential role of the MDTN in thalamocortical dysconnectivity, and ultimately the effect on cognitive function for SZ and BD, all taken together make for not only an interesting area of research, but an opportune intersection for further investigation. Due to the centrality of the MDTN with neuropathology among SZ and BD, great attention has been focused on characterizing its role in the deficits observed in SZ and BD. Taking into account the reductions in neuronal counts, PNN counts, axonal coat counts, nucleus volume, and disrupted thalamocortical activation and connectivity, the investigators employed the techniques of a postmortem investigation to discover if in fact a reduction in cluster counts in the MDTN is associated with disorder diagnosis. Authors then hypothesized lower counts of clusters in the MDTN of tissue slices for people diagnosed with SZ and BD compared to controls.

During the current investigation, high resolution microscopic imaging of the clusters led the authors to find a heterogeneity in the morphology of the clusters that had not previously seen. These morphological differences may correspond to different maturation states of glial clusters during development or learning, or could be differentially affected in people with SZ or BD. However, since a morphological classification had—to the investigators' knowledge—never before been done, the researchers accomplished this in a fact-finding manner while quantifying total numbers and numerical densities of all cluster types. The researchers later analyzed for group differences in classification across diagnoses following data collection.

Summary

In summary, this thesis investigated a neuropathology common to both SZ and BD. Previous investigations from the authors' lab have found novel ECM structures called 6-sulfated chondroitin (CS-6) glial clusters, which consist of 6-sulfated structures associated with glial cells, and are stained by immunoreaction to CS56 antibody. Findings from these investigations indicate CS56-IR clusters may be involved in synaptic regulation. This research team has previously reported marked reductions of these clusters in the amygdalae of persons diagnosed with SZ or BD compared to healthy people. From this, the researchers theorized that glial clusters may be involved in the cognitive and emotional processing deficits suffered by people with psychotic disorders. This thesis sought to extend findings from the amygdala to the MDTN, which was chosen due to its numerous and reciprocal axonal connections with the prefrontal cortex, where imaging studies have shown marked reductions in functional activity and connectivity of persons with SZ and BD.

Support for this link between neuropathology and functional deficits comes from empirical findings of abnormalities in the ECM related to psychiatric illness (Berretta, 2012; Pantazopoulos et al., 2015a; Guidotti et al., 2000). Senior investigators in the authors' lab ran studies on the composition of clusters, finding they are comprised of the same constituents as perineuronal nets (PNNs), and suggesting they potentially serve some regulatory function throughout the intersynaptic domain in kind with PNNs for a single neuron. Although very little is known about the morphology, function, or development of clusters, reductions of these ECM structures have been noted in the amygdalae of people with SZ or BD (Berretta, Pantazopoulos, Markota, Brown, &

Batzianouli, 2015 & Pantazopoulos et al., 2015a). Using postmortem techniques, Pantazopoulos (2015a) showed differences in ECM morphology within nuclei of the amygdala in brain sections from people with a history of SZ and BD. Studying the MDTN will help us to further understand the disruption of this pathway known as thalamocortical dysconnectivity (Jang & Yeo, 2014; Welsh, Chen & Taylor, 2010; Woodward, Karbasforoushan, & Heckers, 2012). As the major hub of sensory input, interpretation and projection to the cortex, the thalamus is of great importance to understanding functional deficits and perceptual dysfunction in SZ and BD. Therefore, the authors examined the cytoarchitecture (brain cell layout) in postmortem tissue slices from three groups of deceased donors, those previously diagnosed with SZ, those with BD, and a third group of healthy control individuals without diagnosis of psychiatric illness. The authors hypothesized that lower counts of CS56-IR clusters would be correlated with people who have been diagnosed with SZ or BD compared to healthy control persons without either diagnosis. This was a blinded, controlled trial.

This data could elucidate a yet undiscovered factor underpinning thalamocortical disruption, thereby explaining the resultant symptomology that is infamous in SZ and BD (Amann et al., 2012; Argyelan et al., 2014; Kahn, 2012; Skåtun et al., 2017). Knowing if ECM cluster changes relate to diagnosis could indicate how people with SZ and BD differ in brain function from unaffected individuals, and whether overlapping perceptual symptoms such as psychosis relate to pathway disruption. Psychopharmacology, therapeutic treatments and diagnostic screening techniques in psychiatry and neuropsychology would be improved with a better understanding of how changes in cytoarchitecture play a role in the cognitive and perceptual dysfunction of SZ and BD.

Chapter II

Method

This study aimed to compare the total number (TN) and numerical density (ND) of CS56-IR clusters in the MDTN of groups of deceased people that had been living with either SZ or BD with that of deceased healthy controls. Total number and numerical densities of clusters in the MDTN, total number of clusters per category, as well as volume of the MDTN, were collected for analyses. The data was collected by computer-assisted quantitative light microscopy after tissue sections containing the MDTN were processed for CS56 immunohistochemistry. We will now detail the population of donors, methods of tissue processing and data collection, and finally, the statistical analyses performed.

Human Subjects

The Harvard Brain Tissue Resource Center (HBTRC) supplied 49 tissue blocks containing whole thalami from a cohort of deceased tissue donors grouped as either: healthy control (*n*=20), person with SZ (*n*=15), or person with BD (*n*=15) (Tables A-1, A-2, and A-3). Whole brain donations were processed on intake for histochemical and immunocytochemical investigations. Retrospective diagnoses of SZ or BD were made based on review of medical records and extensive questionnaires concerning social and medical history, which were provided by family members. A postmortem examination by a forensic neuropathologist and two psychiatrists ensured no tissue blocks contained

evidence of gross and/or macroscopic brain changes, or a clinical history consistent with cerebrovascular accident or other neurological disorders. Donations from persons determined to have had Braak stage III or higher (modified Bielchowsky stain) were not included. No donor had history of substance dependence within 10 years or more of death, and this was verified by toxicology reports. Exclusions for brain abnormalities of donors were made on the evidence of gross and/or macroscopic brain changes, cerebrovascular accident, Alzheimer's, or other neurological disorders. No donor included a history of substance dependence within 10 years of death as evidenced by toxicology reports, as is typical for donations received by HBTRC, as they are received exclusively from the community.

Tissue Processing

Brain intake and tissue processing was handled by the HBTRC located at McLean Hospital, in Belmont Massachusetts. A prescribed protocol for tissue processing was followed (Pantazopoulos et al., 2015a). A table (Table 1) is provided for ease of replication, and a narrative explanation follows below.

Tissue blocks used in this study were processed for immunocytochemistry. First, the blocks were dissected from fresh brains and post-fixed in 0.1 M phosphate buffer containing 4% paraformaldehyde and 0.1 M Na azide at 4 °C for 3 weeks, then cryoprotected at 4 °C for 3 weeks (30% glycerol, 30% ethylene glycol and 0.1% Na azide in 0.1 M phosphate buffer), embedded in agar and pre-sliced in 2 mm coronal slabs using an Antithetic Tissue Slicer (Stereological Research Lab, Aarhus, Denmark). Every slab

Table 1: Tissue Processing Protocol

Step	**Detail**	**Specifications**
1	Tissues are prepared in blocks dissected from fresh brains	post-fixed in 0.1 M phosphate buffer containing 4% paraformaldehyde and 0.1M Na azide at 4ºC for a period of 3 weeks
2	Tissue blocks are then held in a cryoprotectant solution	at 4ºC for another three weeks (30% glycerol, 30% ethylene glycol and 0.1% Na azide in 0.1M phosphate buffer)
3	From here, they are set in agar and pre-sliced	slices conducted in 2 mm coronal slabs with an Antithetic Tissue Slicer (Stereological Research Lab, Aarhus, Denmark)
4	Serialized sections are made with a freezing microtome	(American Optical 860, Buffalo, NY, USA)
5	Finished sections are stored in the same cryoprotectant solution	at -20ºC
6	A system of random sampling is used	40µm thick thalamic sections serially distributed into 26 compartments, 10–12 sections to a compartment, and 1.04mm spacing for sections within each compartment

was sectioned to completion using a freezing microtome (American Optical 860, Buffalo, NY, USA). Sections were stored in cryoprotectant at -20 °C. Using systematic random sampling criteria, sections through the amygdala were serially distributed in 26 compartments (40μm thick sections; 10–12 sections per compartment; 1.04-mm section separation within each compartment). All tissues in all compartments were stained for the histological marker (CS56).

Using CS56 as the primary antibody to stain tissue samples allowed investigators to label and count the clusters under brightfield microscopy. As was discussed earlier in the introduction of this paper, CS56 reliably labels CS-6, the main sulfated sugar chains on ECM macromolecules found on glial processes, axons, dendritic arbors and in the intersynaptic domain. In very concentrated and specific areas, CS-6 reacts immunologically to the CS56 antibody in the shape of what the authors are calling clusters, but have previously been described as dandelion clock-like structures (Harii-Hayashi et al., 2010; Hayashi et al., 2007; Miyata, Komatsu, Yoshimura, Taya, & Kitagawa, 2012 & Pantazopoulos et al., 2015a). Creating CS56-immunoreactive stains was found to be effective in a recent study first identifying the reduction of CS56-immunoreactive clusters in the amygdala (Pantazopoulos et al., 2015a). After staining, 40μm thick serial sections are mounted on glass slides coated in gelatin, then cover-slipped and coded for anonymized analysis. This process is conducted expeditiously to prevent procedural differences with a systemized IHC protocol to preclude any sequencing effects from over-/under-staining any particular set of sections.

Primary Antibody—Histological Marker

CS56: CS56 is a mouse monoclonal IgM (Sigma-Aldrich, St Louis, MO, USA; C8035, lot# 056K4804) made using vertebral membranes from chicken gizzard fibroblasts as an immunogen. The CS structure immunoreactive for CS56 has been identified as an A–D sequence in reducing octosaccharide units on both CS-C (CS-6) and CS-D (CS-2,6) chondroitin sulfate. CS56 has been reported to specifically label CS-6 in brain tissue, and its immunolabeling is virtually absent in CS6ST-1-deficient mice that do not produce CS-6 (Pantazopoulos et al., 2015).

Immunocytochemistry

We achieved antigen retrieval by placing free-floating sections in a citric acid buffer (0.1 M citric acid, 0.2 M Na_2HPO_4) heated to 80 ºC for 30 minutes. Following antigen retrieval, we incubated sections in primary antibody (CS56, 0.25:1000µl) for 48–72 hours at 4 ºC, then placed in biotinylated secondary serum (CS56 goat anti-mouse IgM; 1:500 µl; Vector Labs, Inc., Burlingame, CA). This step was followed by streptavin conjugated with horse-radish perioxidase for two hours (1:5000 µl, Zymed, San Francisco, CA), then a nickel-enhanced diaminobenzidine/peroxidase reaction (0.02% diaminobenzidine, Sigma-Aldrich, 0.08% nickel-sulphate, 0.06% hydrogen peroxide in phosphate buffer). All solutions were made in phosphate-buffered saline with 0.5% Triton X unless otherwise specified.

Sections were then mounted on gelatin-coated slides, cover-slipped, and coated. Each staining dish has six wells and contained sections from SZ, BD and control brains. Each brain in the cohort was processed within the same session, as this avoids procedural

differences, and each staining dish was carried through each step for the same duration of time to avoid sequence effects. This prepares the slides for quantitative analysis, which the authors carried out blinded to diagnosis. Omission of the primary (CS56) antibody did not result in detectable signal.

After slide preparation, data collection occurs in three steps: manually outlining the broad region of the MDTN on each glass slide, electronically drawing the boundaries of the nucleus by computer-assisted light-microscopy using a Zeiss Axioskop 2 Plus interfaced with Stereo Investigator (v. 10.54; Microbrightfield Inc., Willinston, VT) (which also yields the computable area of the nucleus on all slides, from which the authors can extrapolate volume of the MDTN), then, counting total number and density of clusters within the boundaries drawn by labeling clusters using the Stereo Investigator software.

Characterization of the MDTN

Using Stereo Investigator software, virtual tissue (montage) scans of CS56 stained sections were taken at 2.5X magnification to identify cytoarchitectonic changes between subnuclei within the MDTN and around it. Manual dotting on the cover-slipped glass slides roughly and conservatively outlined the MDTN, if present, in each section for all donors. Following that, computer-assisted electronic tracing delineated the official boundary lines of the MDTN wherein the researchers counted. To confirm boundaries, adjacent sections from within the same series of slides—that were sliced just before (rostrally) or behind (caudally), but stained in either Nissl or Luxol Fast Blue (LFB) for

other studies—were thoroughly examined to verify section positioning for ultimately estimating volume (Figure 1).

Data Collection

Total numbers of all clusters and cluster categories, as well as numerical densities of clusters and volume of the MDTN were collected using the following methods. Intra-rater reliability of at least 95% was established before officially recorded counting began, and was assessed regularly throughout data collection. Every cluster within the electronically traced boundary was counted, as the clusters are too large and distributed too heterogeneously or sparsely throughout the tissue to meet the fundamental criteria for stereology (Figure 2).

During quantification, the MDTN in each section was traced as a "live" image, first at low magnification (2.5X) on the basis of landmarks, then confirmed at high magnification (40X) based on cytoarchitectonic gradients consistent with thalamic or subthalamic nuclei known in histology. All MDTN traced were done using the full X, Y and Z axes. Numerical densities (ND) were calculated by using the following equation: $ND = \sum N / \sum V$, where N is the sum of clusters within a region and interest, and V is the total volume of the region of interest. Total number (TN) of CS56-IR clusters was calculated using the following equation: $N = i(\sum n)$, where $\sum n$ is the sum of the cells counted in each subject, and i is the section interval, or the number of serial sections between each section and the next within each compartment (26 compartments), as described previously in Tissue Processing.

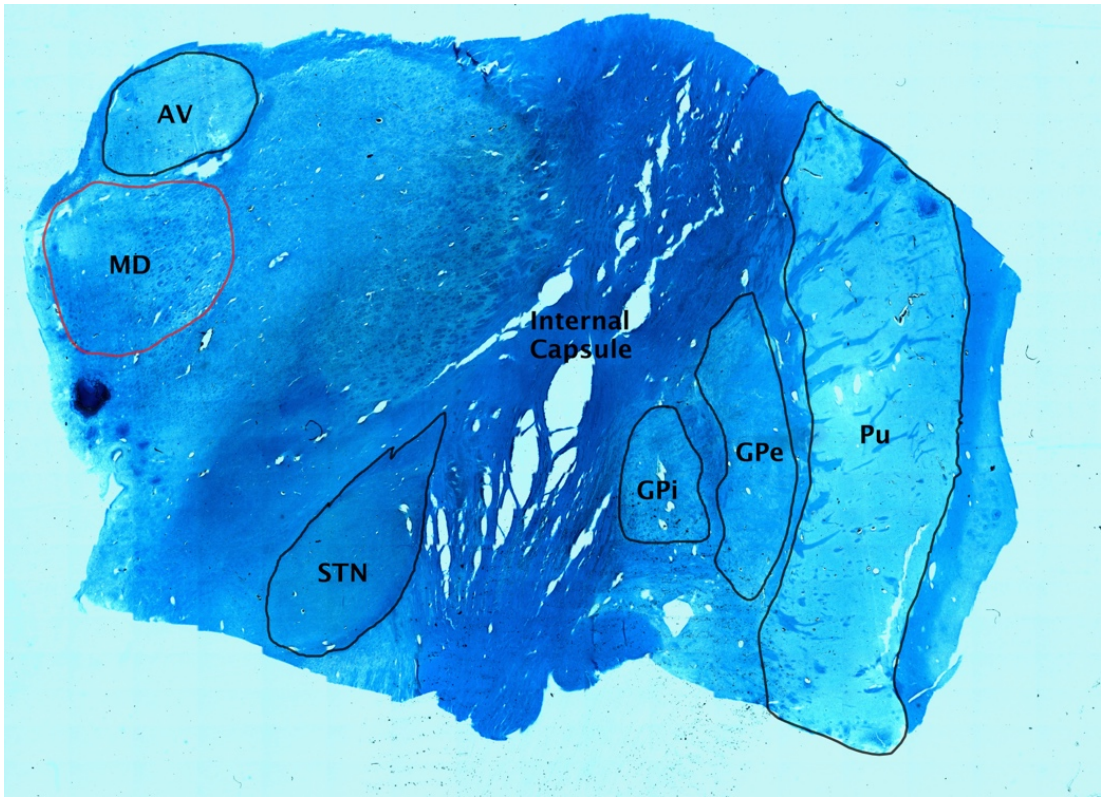

Figure 1: Virtual tissue montage of human thalamus. Coronal section scan of thalamus at 2.5X magnification. Stained in Luxol Fast Blue. Anteroventral (AV) Nucleus, Mediodorsal (MD) Nucleus, Subthalamic Nucleus (STN), Internal Capsule, Globus Pallidus-internal (GPi), Globus Pallidus-external (GPe), & Putamen (Pu).

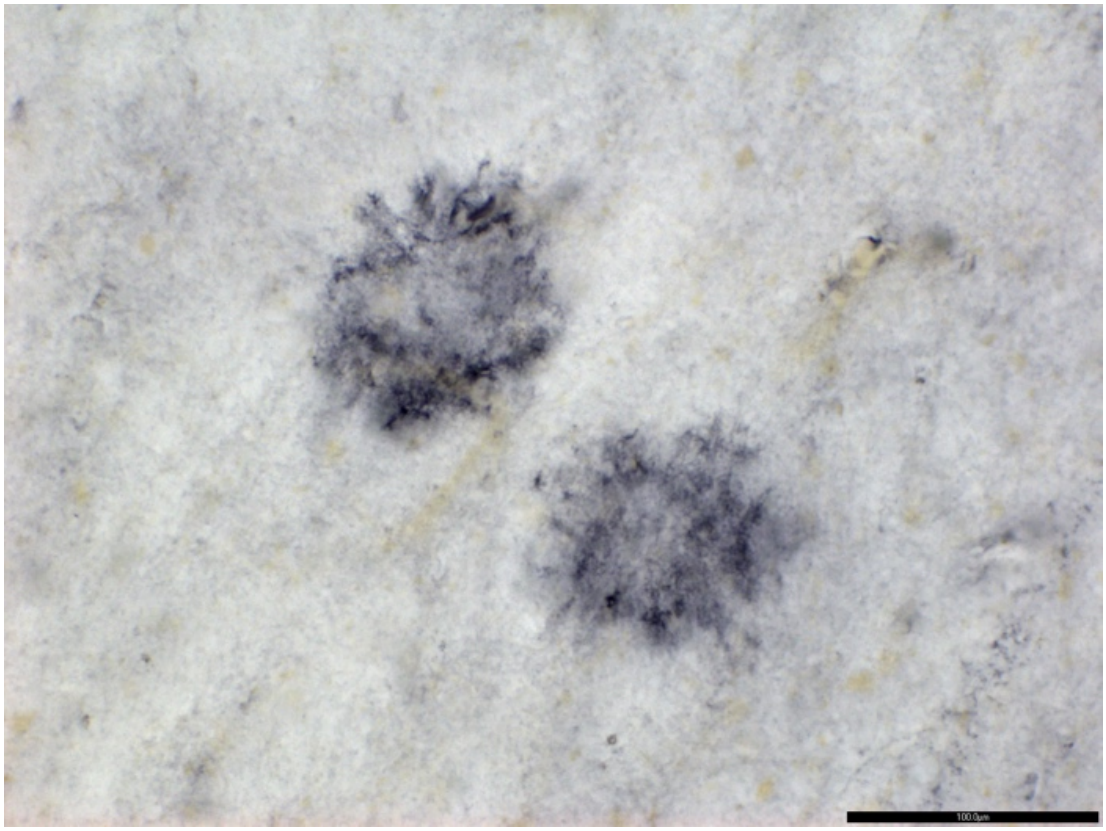

Figure 2: Two CS56-IR clusters in MDTN. 20X magnification. Scale bar, 100µm.

Cluster Categories

As was previously discussed, high resolution imaging in this study led the authors to find distinctions in CS56-IR cluster morphology indicating heterogeneity not previously seen. On the basis of the typical morphological characteristics observed, the authors developed a set of criteria including size, shape, and staining intensity to divide these structures into distinct categories. Sizes ranged from 50μm–220μm in diameter. Shapes including circular, ovular, and amorphous were counted only if the structures could be circumscribed within the diameter of size criteria. CS-6-stained intensity of a cluster must have been at least twice the intensity of background tissue. The most prominent characteristic of a cluster was then used to classify its category: *fibrous*, *diffuse, densely diffuse*, and *type-4*. Fibrous-types must include at least three sharply stained tendrils, and may exhibit a hollow center with diffuse staining throughout (Figures 3 and 4). Diffuse-types must be diffusely stained, may or may not exhibit a hollow center, and may have at most two tendrils (Figures 5 and 6). Densely diffuse-types must be quadruple the intensity of background, and exhibit the same shape as normal fuzz (Figures 7 and 8). Type-4s must have minimum three densely stained patches of CS-6 labeling not connected by fibrous tendrils (Figures 9 and 10). All types co-localized in one image can seen in Figure 11.

Statistical Analysis

This was a blind, retrospective investigation. ANCOVA stepwise linear regression was used to assess statistical significance for differences relative to the main outcome measures between groups. The researchers used Hedges' *g* to calculate effect

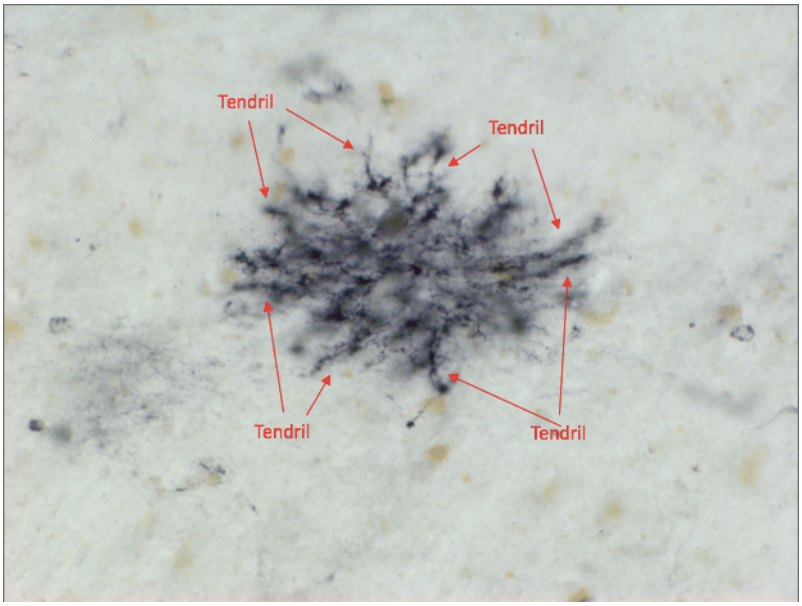

Figure 3 (top): Tendril Type, Example 1 (40X)

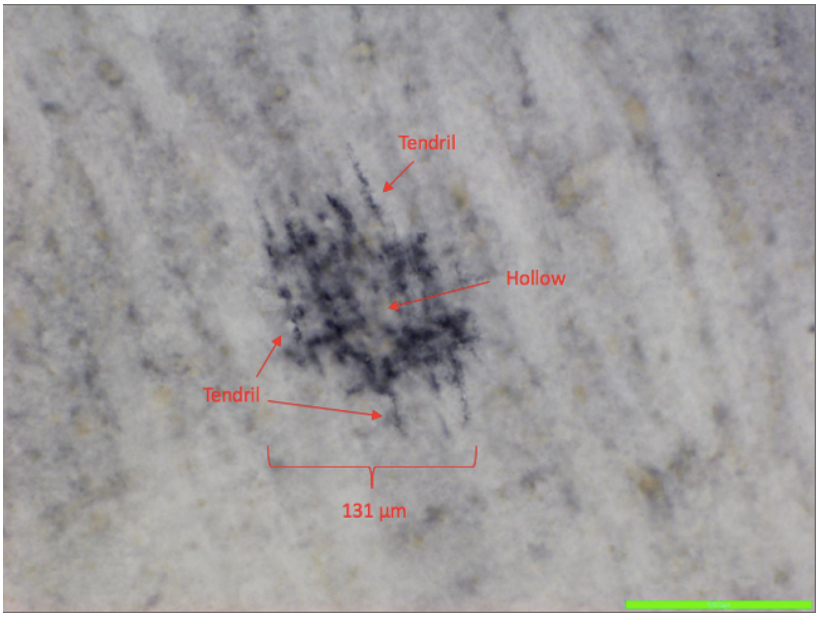

Figure 4 (bottom): Tendril Type, Example 2 (20X, scale bar represents 100µm)

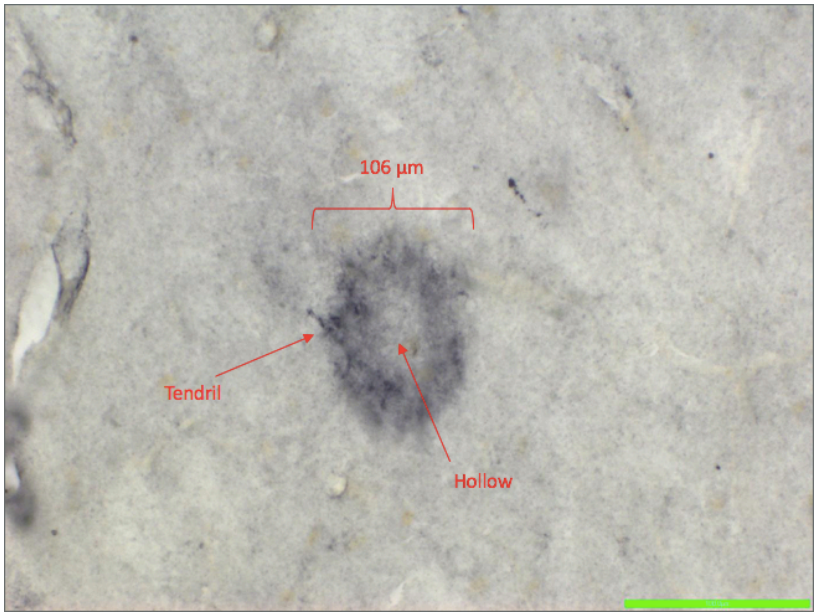

Figure 5 (top): Diffuse Type, Example 1 (20X, scale bar represents 100µm)

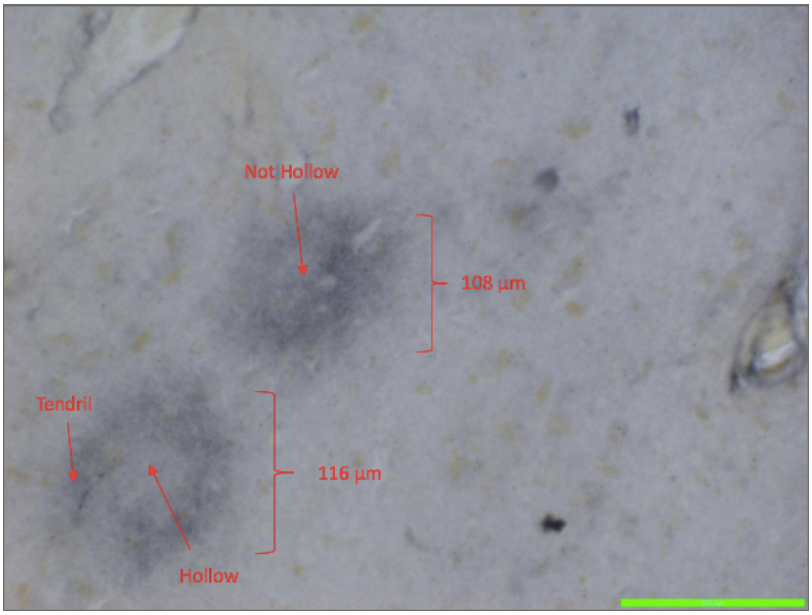

Figure 6 (bottom): Diffuse Type, Example 2 & 3 (20X, scale bar represents 100µm)

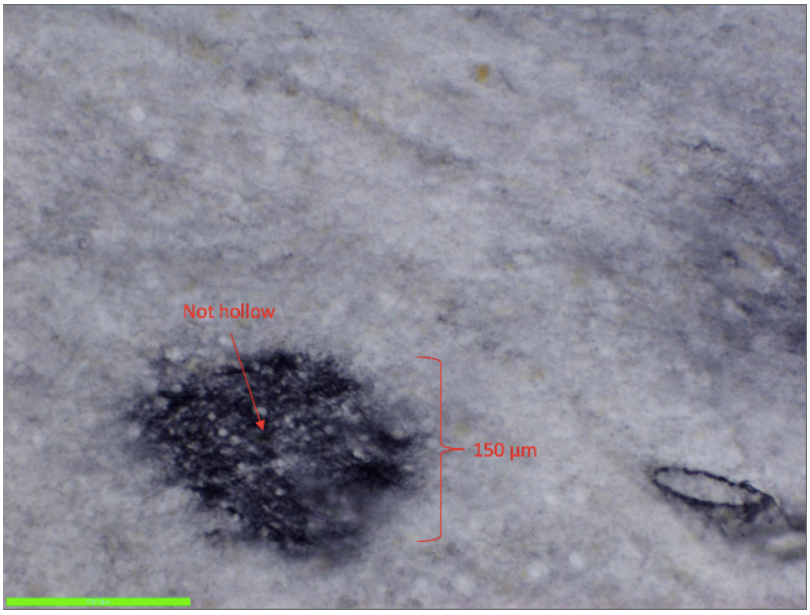

Figure 7 (top): Densely Diffuse Type, Example 1 (20X, scale bar represents 100µm)

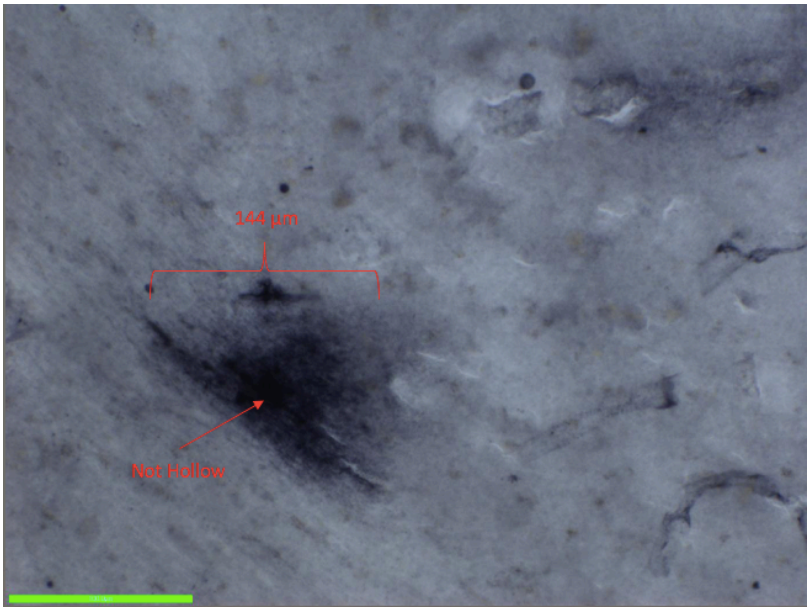

Figure 8 (bottom): Densely Diffuse Type, Example 2 (20X, scale bar represents 100µm)

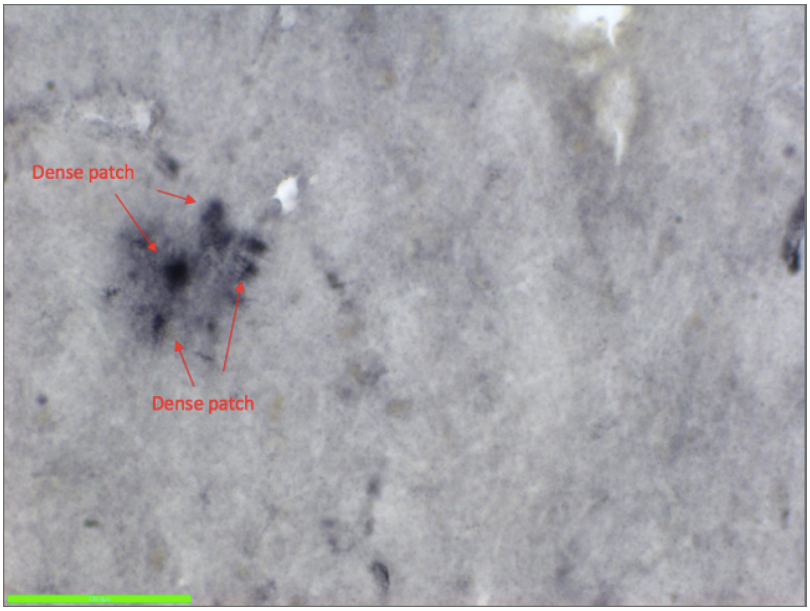

Figure 9 (left): Type-4, Example 1 (20X, scale bar represents 100µm)

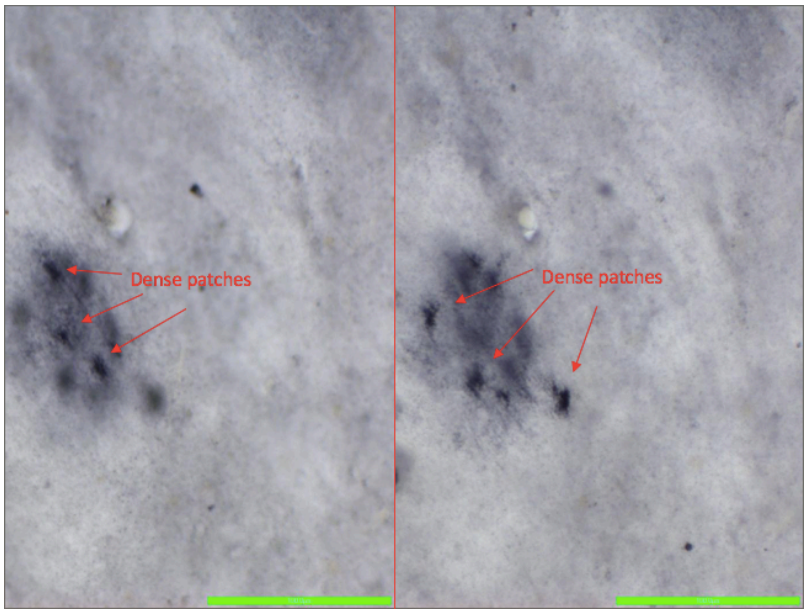

Figure 10 (right): Type-4, Example 2 (same cluster shown in two focal planes; 20X, scale bar represents 100µm)

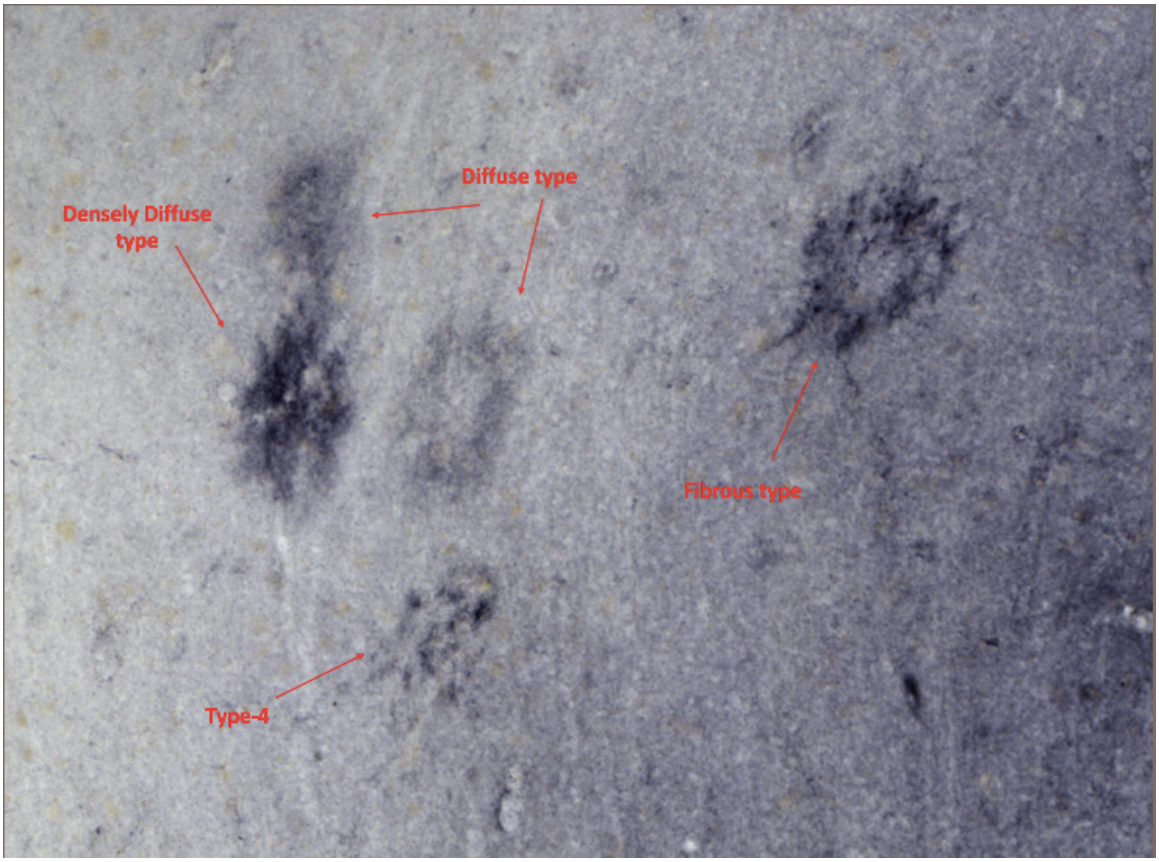

Figure 11: All four cluster types (two diffuse types, one densely diffuse type, one tendril type, one type-4; 10X, scale bar represents 100µm)

sizes. They then applied a logarithmic transformation uniformly to all original values in order to better homogenize the data, which was not normally distributed. This was typical and to be expected for postmortem data. Keeping with convention, this method of analysis was used and detailed in prior studies from the authors' lab (Pantazopoulos et al., 2010 & Pantazopoulos et al., 2015a).

The authors performed their analyses using JMP v5.0.1a (SAS Institute., Cary, NC). SZ and BD were independently compared to healthy controls. Variables included age, duration of illness, gender, postmortem time interval, hemisphere, brain weight, electroconvulsive therapy, lifetime exposure to antipsychotic drugs, final six month's exposure to antipsychotic drugs, history of selective serotonin reuptake inhibitors (classified as positive or negative for exposure), lithium treatment, cause of death, history of alcohol exposure, and history of nicotine use (Tables 1, 2-1, and 2-2). The investigators tested these variables as covariates in the ANCOVA model in a systematic manner in order to assess their effects on the main outcome measures, and included them in the model if they significantly improved the model goodness of fit. Both patient group's exposure to pharmacological agents was calculated by extensive review of medical records to estimate lifetime cumulative exposure to relevant classes of psychotropic and neurotropic drugs. Authors report these values in Table 2 as lifetime, as well as last six months of life, in grams per patient. To estimate patients' exposure to antipsychotics and antidepressants, investigators converted estimated daily doses (in mg) of the drugs they took into the approximate equivalent dose of standard comparators (i.e. chlorpromazine as the antipsychotic and imipramine as the antidepressant). For treatment-adherence, investigators qualitatively coded medical compliance as "good" or

"poor," and based this on an extensive review of antemortem clinical records for whether or not prescribed psychotropic medicines were taken roughly half the time. Cause of death was coded as acute (e.g. myocardial infarction) or chronic (e.g. cancer) in Table 1. Alcohol and nicotine usage data was available only for SZ and BD medical records; exposure for these as well as electroconvulsive therapy exposure was coded on a Likert scale (low-1 to high-5). Again, the authors present these covariates and the raw data for them in Table 2. However, some variables, including subtypes of SZ (e.g. catatonic, paranoid and disorganized) and quality of life (e.g. dependent/independent), could not be included in formal statistical analyses due to the modestly low number of donor cases available in the cohort, however, they were taken into account as a possible explanation of clustering among subjects when results presented as such. See Sullivan et al. (2017) for a detailed description of how medical records were used to obtain information for covariates.

Chapter III

Results

The main thrust of this investigation was to determine if a significant relationship exists between quantities of CS56-IR clusters in the MDTN and whether or not a person has a diagnosis of either SZ or BD. This will ultimately allow researchers to draw inferences about the role clusters play in the neuropathology of SZ and BD, which can serve as the foundation for subsequent tests of causality to symptoms, then potential drug targets for therapy. Authors present their results in this Chapter, and continue with a discussion of what this means for the field and for persons suffering psychosis in Chapter IV.

TN and ND data were log transformed in statistical analyses to homogenize the data, as postmortem data is often highly heterogeneous. The investigators hypothesized that diagnosis of either psychotic disorder would correlate with total number of CS56-IR clusters, and this relationship was significant for both SZ ($p<0.04$) and BD ($p<0.005$) compared to healthy controls. Investigators hypothesized that diagnosis of either psychotic disorder would correlate with numerical density of CS56-IR clusters, and this relationship was significant for both SZ ($p<0.02$) and BD ($p<0.03$) compared to controls. To ensure the reduction of cluster counts was not due to a difference in brain mass across groups, investigators analyzed the relationship of MDTN total volume to diagnosis, and found this relationship was not significant for SZ nor BD compared to controls. Using ANCOVA, investigators found a significant correlation between total number of clusters

with SZ diagnosis compared to controls, when using CPZ in the last six months as a covariate ($p<0.005$), but this relationship was not found for BD compared to controls. Investigators also found a significant correlation between numerical density of clusters with BD diagnosis compared to controls, when using CPZ in the last six months as a covariate ($p<0.05$), but this covariate relationship was not significant for SZ. Finally, the investigators found a significant correlation between total number of clusters with SZ diagnosis compared to controls, when using duration of illness as a covariate ($p<0.03$, $R^2=0.34$), but this covariate relationship was not significant for BD. Findings are graphically presented in Figure 12 below, and a JMP statistical output for the model of TN and duration of illness is presented in Chapter IV.

No other covariates for SZ or BD had any significant main effects. Investigators ran an ANCOVA for age, gender, postmortem time interval, hemisphere, brain weight, electroconvulsive therapy, selective serotonin reuptake inhibitor exposure, lithium treatment, cause of death, history of alcohol exposure, and history of nicotine use. No significant effects were found for statistical models using these covariates. When analyzing the cluster categories with the diagnoses, we found no significant effects, only with total number, across all cluster types, was there a significant effect of diagnosis compared to healthy controls. The authors discuss what this potentially means for the field and for persons suffering psychosis in the final chapter of this thesis.

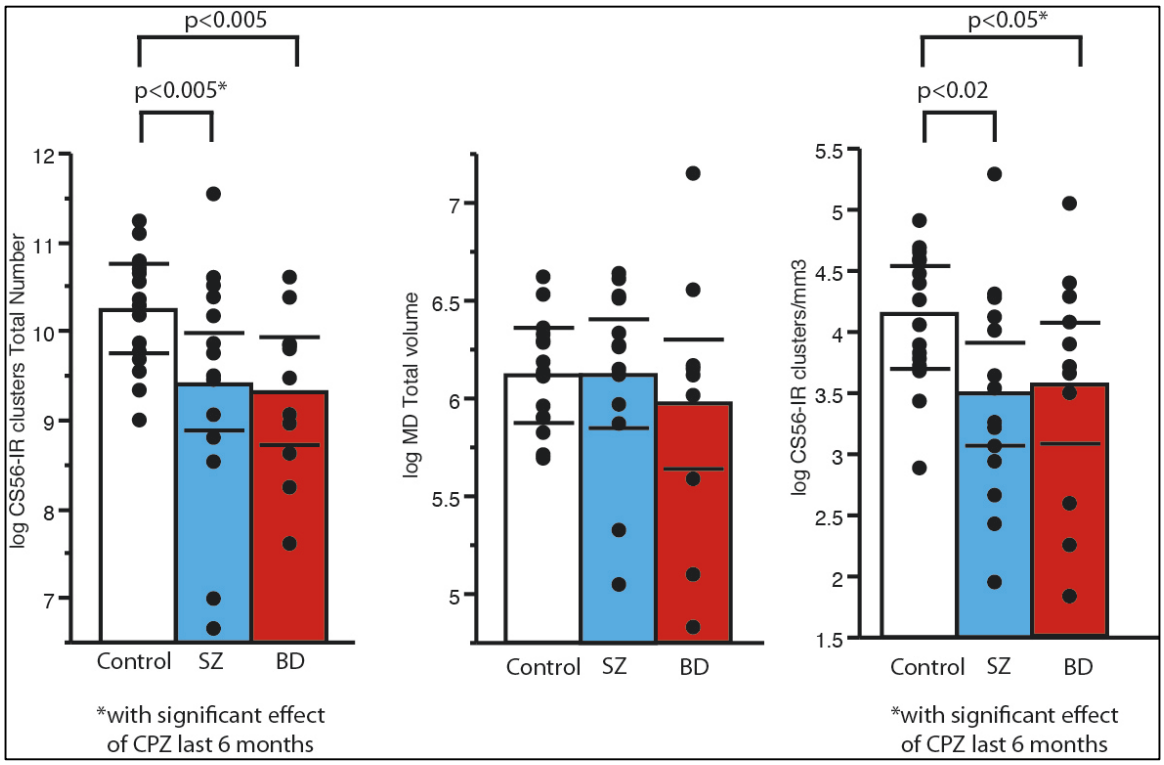

Figure 12: Quantification of CS56-IR Clusters in the MDTN – Total Number of CS56-IR Clusters vs. Diagnosis (left), Total Volume of MD vs Diagnosis (middle), Density of CS56-IR Clusters vs. Diagnosis (right)]

Chapter IV

Discussion

This thesis began with first identifying the clinical pictures of SZ and BD as major psychoses afflicting sufferers' and their loved ones' quality of life, outlining the history of disease management, and describing the modern day study of their etiology and pathology. After detailing the brain regions of interest for investigation into a neurobiological cause of thalamocortical dysconnectivity as the structural degradation potentially responsible for the cognitive and emotional processing deficits of SZ and BD, it then discussed the main interest of changes in a new ECM structure, the CS-6 glial cluster, that the authors believe could be a missing, integral role in what should otherwise be healthy brain function. The authors hypothesized these clusters would be reduced in the region of interest, the MDTN. Here, this thesis concludes with a discussion and interpretations of those findings.

Results of the present investigation support the investigators' hypotheses that both total numbers (TN) and numerical densities (ND) of CS56-IR clusters in the MDTN of patients with either SZ or BD were quantifiably reduced compared to samples analyzed from donors in the control group. The main effect of total volume of the MDTN with a diagnosis of either psychotic disorder was not significant compared to controls. This was unremarkable, as the investigators' inclusion requirements ensured all cohort brain samples included no evidence of macroscopic brain trauma in the neuropathological

forensic report. One interpretation the authors offer is that the brains of persons suffering SZ or BD develop normal structurally, but aberrant functionally.

Because this study examines the tissues of people with documented diagnoses, prescribed medications could have posed potential confounds to cytoarchitecture. Therefore, medication history was considered as a covariate, as the observed brain tissue differences could be due to long term exposure to antipsychotic medications rather than the underlying psychopathology. Investigators found no significant correlation when testing this as a covariate. Other potential confounds such as sex, medication, age, postmortem interval, etc. were also considered, and similarly investigators found no significant relationships.

The one effect on BD for which investigators did find significance occurred for BD diagnosis with cluster ND, which as a main effect yields a p-value of 0.05. An ANCOVA of lifetime CPZ in grams (g) exposure was not significant, but when using CPZ in g within the last 6 months as a covariate, the ANCOVA returned with a p-value of 0.05, showing that some of the variance is explained in the model when including CPZ exposure for the last six months of life, but not enough to completely negate the main effect of BD diagnosis with CS56-IR clusters numerical density. If amount of CPZ exposure in the last six months were correcting the deficit of lowered clusters for individuals diagnosed with BD compared to controls, then the authors would have expected to find no significant effect when accounting for CPZ usage in the last six months as a covariate. However, one limitation to interpretation of this result is that this effect was mostly driven by the data collected from one donor with more than five times the dosage of CPZ in the last six months than any other donor in the BD group. The main

effect of SZ diagnosis with cluster TN was as well significant when using the ANCOVA with CPZ in g within the last six months as a covariate. Again, this was significant without the covariate, showing that CPZ usage potentially explains some amount of variance, but not enough to correct the reduction of total number of clusters in persons with SZ compared to controls.

The covariate relationship of a diagnosis of SZ to TN with duration of illness was significant ($p<0.05$, $R^2=0.34$), although not found for BD (Table 2). A graphical output of relationship is shown in the JMP output below (Figure 13). A possible interpretation of this findings is that age of persons with SZ, or more years of a psychiatric pathology unique to SZ, reduces cluster counts in a way that is preserved in BD. This would mean a difference in the potential underlying pathology causing for a more deleterious effect for duration of illness in SZ with TN of clusters, but not in BD. Clinical investigations and pharmacological trials might then be directed toward a method of detection of this pathological signature for SZ compared to BD in order to protect against this degenerative process. Subsequent work based on the present findings could offer insight to further support functional imaging and other clinical means of diagnostics. Finding a link between neuropathology and psychiatric diagnosis could advance an understanding of cognitive and emotional deficits among people with major disorders such as SZ and BD.

Table 2

Bivariate Fit of log CS56 Combined Clusters TN by Duration of Illness

Linear Fit

log CS56 combined clusters TN = 11.692755 – 0.0572215*duration of illness

Summary of Fit	RSquare	RSquare Adj	Root Mean Square Error	Mean of Response	Observations (or Sum Wgts)
	0.344121	0.289464	1.139519	9.420245	14

Analysis of Variance

Source	DF	Sum of Squares	Mean Square	F Ratio
Model	1	8.175454	8.17545	6.2961
Error	12	15.582050	1.29850	Prob > F
C. Total	13	23.757504		0.0274*

Parameter Estimates

Term	Estimate	Std Error	t Ratio	Prob>ltl
Intercept	11.692755	0.955507	12.24	< .0001*
duration of illness	-0.057221	0.022805	-2.51	0.0274*

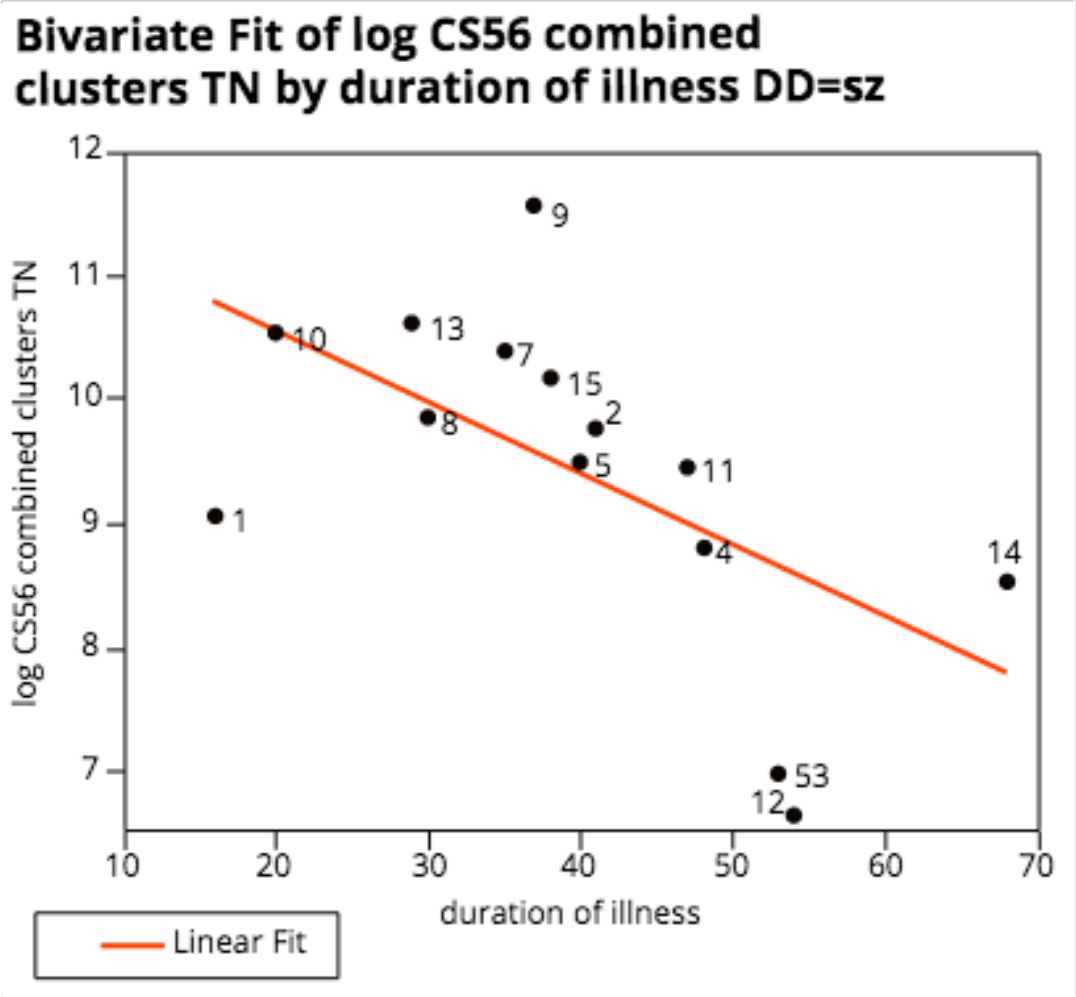

Figure 13: Cluster total number by duration of illness (SZ)

When analyzing the four cluster categories with the diagnoses, investigators found no significant effects. Only with total number, across all cluster types, was there a significant effect of diagnosis compared to healthy controls. Importantly, authors suspect these cluster categories are not differentially affected in either a diagnosis of SZ or BD compared to controls for the reason that they are equally effected at the same time point. To explain in another way, should the four categories of clusters prove to be developmental stages, then a reduction in total number and numerical density would sensibly result in fewer clusters developing through the life cycle, while the cluster life cycle itself would remain largely unaffected. This is consistent with investigators' results, and future studies in their lab will seek to explore this developmental trajectory.

The quantification carried out in this investigation established the distribution of four categories of cluster morphology in the human MDTN. Future investigations in rodents will examine a temporal aspect of the cluster morphology. Researchers from their lab may investigate if categories are indicative of temporal development, specifically, if they are neurodevelopmental (i.e. lifelong) or cross-sectional (continuing throughout the lifespan) in response to behavioral learning and memory consolidation. This will allow a comparison of morphological cluster categories and functional regulation of synaptic plasticity following fear learning and in other rodent models of cognitive or emotional dysfunctions from SZ and BD.

Postmortem studies often run a high risk of type II error due to small sample size and often weak statistical power (Meurs, 2016). While samples can typically be single digit in number to a roughly a dozen, this investigation enjoyed a relatively large cohort size of 49 cases of donated brain tissue. As well, minimizing the number of factors

analyzed allowed the present investigators to retain as much statistical power as possible with the linear regression models and the ANCOVA models (Popken et al., 2000). The researcher conducting the slide preparation, staining, counting, and analysis was blinded to donor identity, and did not know whether the tissue slices from any person being examined belonged to either a diagnosis or control group until data collection was complete.

An inherent limitation of postmortem studies is the inability to draw casual inference from results and generalizability to a living population. However, the high resolution of examination available by microscopy—on the order of microns compared to structural MRI imaging on the order of millimeters—offers a clear and obvious benefit to conducting the examination in postmortem tissue samples. This method made possible an evaluation of whether ECM differences are associated with the brain changes in SZ and BD observed in imaging studies. Another limitation to postmortem work is that samples are from an aged population (66.21, mean age of all diagnosed donors, 64.23 for all donors including controls). This limits these researchers' ability to generalize to changes in early brain pathology with results potentially reflecting effects after decades of brain illness.

As detailed in Chapter I, clusters are a structure comprised of ECM macromolecules, CSPGs. As were found with changes in PNNs, another well-known ECM structure, authors believe these changes found in clusters indicates their participation in neurotypical cognitive and emotional function, that when reduced in number, potentially due to CSPG abnormalities, contribute to the clinical picture of

psychosis. Gene polymorphisms, deficiencies in glycoproteins, dysregulation of glutamate transmission are all examples of CSPG dysfunction.

Okuda et al. (2014) recently confirmed clusters are produced by astrocytes by showing co-localization of CS56 and a mature astrocyte marker called S100ß. They argue for a linked relationship of cluster development to the functional maturation of astrocytes as regulated by glutamate transporters expressed by the astrocytes. Astrocytic expression of glutamate transporters ramps up postnatally during the same period when clusters appear to develop in the cortices (Okuda, et al., 2014). Authors believe this supports their suspicions of cluster involvement in cognitive processing deficits in SZ, which is typified by dysfunctional glutamate transmission.

An interesting study by Matuszko et al. (2017) examined ECM alterations in a rodent model of SZ. Inducing the negative symptoms of SZ in rats by subchronic administration of ketamine resulted in a significant decrease of the number of PNNs in the medial prefrontal cortex, as well as an increase of antibody intensity of CS-6 expression, and therefore, CS56-immunofluorescent cluster expression compared to control rats—though numerical density of clusters held consistent. The authors contribute the higher intensity of cluster expression in the ketamine-induced SZ group to state changes in glial cells, which makes for interesting potential that pharmaceutical trials could explore to develop molecular modulation of the ECM as a therapeutic intervention for negative symptoms.

Finally, the authors conclude that findings of quantifiably reduced clusters in SZ and BD support an ever expanding knowledge base detailing the disruption of CSPGs as a core feature of psychiatric illness, SZ in particular (Pantazopoulos & Berretta, 2015).

Gene variants responsible for CSPG development are associated with SZ and BD, and both diseases are known to have altered levels of matrix metalloproteases responsible for regulation of synaptic plasticity. Rodent models of pharmacological disruption of matrix metalloproteases result in cognitive and emotional deficits similar to those seen clinically in persons with SZ and BD (Berretta et al., 2015; Pantazopoulos & Berretta, 2015). These findings have been consistent with reduced numbers of PNNs in SZ and BD as well as other major psychiatric illnesses, and we suspect the mechanisms responsible for the reduction in PNNs may contribute to the reduction in clusters seen in this present investigation.

As with many findings in neuropathology, these results suggest cluster quantifications are a relatively useful association of biological underpinnings with psychological states, but cannot currently be used in daily psychiatric screenings or developed into rehabilitation therapies. As was discussed, brain imaging cannot detect these molecular changes on the scale of microns, and if such a machine could, an association alone could not be used as a diagnostic aid. The utility of the authors' findings, then, represents an immediate benefit to the scientific community. They have found that psychiatric illness has a quantifiable relationship to reductions in CS56-IR clusters, which supports the rapidly growing evidence surrounding similar abnormalities for other CSPG structures. However, this should embolden researchers to continue honoring the contribution of brain tissue donors and their families, and helping our fellow woman and man living with these psychiatric illnesses by reporting findings such as these to the field. The authors aim next to confirm what role specifically clusters play in contributing to the cognitive and emotional deficits of brain diseases such as SZ and BD.

Appendix A

Table A-1: Sample Demographic and Descriptive Characteristics

Case	Age	Sex	Cause of death	brain weight (g)	PMI (hrs)	Hemisphere
Schizophrenia						
S09222	32	M	Cardiac Arrest and Pancreatitis (A)	1400	7.8	L
S13800	61	F	Pneumonia (A)	1200	14.1	R
S08533	73	F	Cardiac Arrest (A)	NA	32	R
S03424	72	F	Renal Failure (C)	1065	21.75	L
S11396	61	F	Cardiac Arrest (A)	1135	11	L
S18002	56	F	Cancer (C)	1185	18.7	R
S07414	80	M	Cancer (C)	1440	10.97	R
S16818	54	F	Cardiac Arrest (A)	1280	32.6	R
S05622	55	M	Cardiac Arrest (A)	1380	21.4	L
S10393	63	M	Cancer (C)	1370	22.4	L
S14112	73	F	Cancer (C)	1130	28.8	R
S14599	49	M	Cardiac Arrest (A)	1460	24.5	L
S08862	92	F	Cardiomyopathy (A)	1120	17.8	L
S02133	58	M	COPD (C)	1160	32.38	R
S11020	49	M	Suicide (A)	1440	19.1	R
Total/ mean ± SD	61.9 ±14.6	8F 7M		1268.9 ±141.3	20.0±8.0	7L 8R
Bipolar Disorder						
S17334	78	F	Cardiac arrest (C)	1170	22.8	R
S00956	73	M	Pneumonia (A)	1190	7.2	R
S00096	67	F	Pneumonia (A)	1150	25.3	L
S01970	50	M	Cancer (C)	1360	30.5	L

S15500	74	M	Pneumonia (A)	1270	24.8	L
S10576	66	M	Pneumonia (C)	1480	17.4	R
S19900	73	F	Sepsis (C)	1060	20.8	L
S16699	74	M	Pneumonia (C)	1340	14.3	R
S17401	73	F	Cancer (C)	1020	17	L
S03567	83	M	Systemic infection (C)	860	17.5	L
S09588	47	F	Unknown	1000	16.3	L
S05487	41	M	Suicide (A)	1385	30.75	R
S09786	25	M	Pulmonary edema (A)	1480	12.56	R
S19702	79	F	Cancer (C)	1085	22.6	R
S17705	70	M	Renal Failure (C)	1215	17.25	L
Total/mean ± SD	64.7± 16.4	6F 9M		1204.3± 182.3	19.8±6.5	8L 7R
Controls						
S05735	74	F	Cancer (C)	1145	12.2	L
S16022	68	F	Cardiac Arrest (A)	1330	14.75	R
S13845	37	M	Electrocution (A)	1460	18.75	R
S14247	72	M	Cardiac Arrest (A)	1560	28.2	R
S10160	85	M	Cancer (C)	1225	20.3	L
S18228	78	F	Cancer (C)	1100	23.9	L
S07594	95	F	Unknown	1350	7.1	R
S06087	69	F	Unknown	1280	25.2	R
S07749	61	M	Unknown	1280	10.1	R
S07429	68	F	Unknown	1230	24.8	R
S14342	70	F	Cardiac Arrest (A)	1245	18	R
S08468	26	M	Unknown	1250	18.3	R
S08987	53	F	Cancer (C)	1330	24	R
S11774	74	M	Cardiac Arrest (A)	1490	15.81	R
S03774	70	M	Aortic Aneurysm (A)	1400	17.3	R
S17165	58	F	COPD (C)	1345	17.8	R
Total/mean ± SD	66.1±16.8	9F 7M		1313.8± 122.1	18.5±5.8	3L 13R

Abbreviations: A, acute death, no prolonged agonal period; C, chronic, prolonged agonal period; COPD, Chronic Obstructive Pulmonary Disease; PMI, postmortem time interval

Table A-2: Disease-Related Descriptive Statistics (SZ)

case	S10393	S05622	S16818	S07414	S18002	S11396	S03424	S08533	S13800	S09222
SCHIZOPHRENIA										
Age at Onset	16	35	17	50	21	21	24	20	20	16
Duration of illness (years)	47	20	37	30	35	40	48	53	41	16
CPZ (g)	1019.2	793	184.5	801.5	3896	410.9	420	750.5	3550	671
last 6 months (g) CPZ	18	27	0	36	36.1	20.3	31.5	3.4	36.2	30
LI (g)	0	0	54	0	0	0	0	1095	0	0
last 6 months (g) Li	0	0	0	0	0	0	0	0	0	0
nicotine	0	1	-	-	-	-	1	0	2	3
ethanol	0	1	-	-	-	3	0	0	2	2
ECT	0	2	-	2	-	3	0	0	3	0
SSRI	Yes	Yes	No	No	No	Yes	Yes	No	Yes	No
VPA (g)	0	0	0	0	3250	0	0	0	0	0
ADP (g)	12775	346.75	0	0	0	146	109.5	0	5475	0

S11020	S02133	S08862	S14599	S14112
19	20	24	20	19
30	38	68	29	54
801.5	2430	0	1668	37
36	81	0	51.4	0
0	648	0	0	36.8
0	108	0	0	0
1	3	-	5	2
2	-	-	5	0
2	0	-	0	0
No	No	No	No	No
913.1	730	0	0	0
0	0	0	9000	0

See notes for Tables A-2 & A-3 following Table A-3.

Table A-3: Disease-Related Descriptive Statistics (BD)

case	S17401	S16699	S19900	S10576	S15500	S01970	S00096	S00956	S17334
BIPOLAR DISORDER									
Age at Onset	35	18	20	35	52	34	23	30	67
Duration of illness (years)	38	56	53	31	22	16	44	43	9
CPZ (g)	82.2	2842	202.7	731.3	102.5	200	237.5	10.8	77.9
last 6 months (g) CPZ	20.3	150	13.9	1	29.3	20	54	3.6	2.7
LI (g)	2191.5	2192	4273	1096	3945	1000	4131	0	1321
last 6 months (g) Li	0	350	0	54	0	50	0	0	27
nicotine	0	-	1	4	1	3	4	1	4
ethanol	0	-	0	0	2	2	2	0	3
ECT	0	-	0	0	0	-	3	0	0
SSRI	No	No	No	No	No	No	No	No	No
VPA (g)	182.6	1825	0	0	547.9	0	1825	0	0
ADP (g)	21425	0	0	0	0	0	585.8	0	-

	S17705	S19702	S09786	S05487	S09588	S03567
Age	27	22	15	17	18	43
Age at onset	43	57	10	24	29	40
ADP	0	430.8	328.7	465.4	64.2	0
CPZ	0	0	90	49.5	40.3	0
CPZ last 6	3240	1752	3945	135	8547	2190
ECT	0	0	216	0	0	0
Ethanol	4	-	3	-	-	-
LI	4	-	2	5	3	0
LI last 6	3	4	0	5	-	0
Nicotine	No	Yes	Yes	Yes	No	Yes
SSRI	456.3	0	0	0	5694	803.6
VPA	65.7	619.6	-	470.9	0	-

Abbreviations: ADP, lifetime exposure to antidepressants (in grams - normalized to imipramine equivalent); CPZ, lifetime exposure to antipsychotics (in grams - normalized to chlorpromazine equivalent); CPZ last 6, last 6 months' of life exposure to antipsychotics (in grams - normalized to chlorpromazine equivalent); ECT, electroconvulsive therapy (low 1 to high 5); Ethanol exposure (low 1 to high 5); LI, lifetime exposure to lithium (in grams); LI last 6, last 6 months' life exposure to lithium (in grams); SSRI, exposure to selective serotonin reuptake inhibitors; Nicotine exposure (low 1 to high 5); VPA, lifetime exposure to valproic acid (in grams)

References

Aleman, A., & Kahn, R. S. (2005). Strange feelings: Do amygdala abnormalities dysregulate the emotional brain in schizophrenia? *Progress in Neurobiology*, *77*(5), 283–298. https://doi.org/10.1016/j.pneurobio.2005.11.005

Amann, B., Gomar, J. J., Ortiz-Gil, J., McKenna, P., Sans-Sansa, B., Sarró, S., … Pomarol-Clotet, E. (2012). Executive dysfunction and memory impairment in schizoaffective disorder: a comparison with bipolar disorder, schizophrenia and healthy controls. *Psychological Medicine*, *42*(10), 2127–35. https://doi.org/10.1017/S0033291712000104

American Psychiatric Association. (2013). Diagnostic and statistical manual of mental disorders (5th ed.). Arlington, VA: American Psychiatric Publishing.

Andreasen, N. C., Paradiso, S., & O'Leary, D. S. (1998). "Cognitive Dysmetria" as an Integrative Theory of Schizophrenia. *Schizophrenia Bulletin*, *24*(2), 203–218. https://doi.org/10.1093/oxfordjournals.schbul.a033321

Anticevic, A., Cole, M. W., Repovs, G., Murray, J. D., Brumbaugh, M. S., Winkler, A. M., … Glahn, D. C. (2014). Characterizing thalamo-cortical disturbances in Schizophrenia and bipolar illness. *Cerebral Cortex*, *24*(12), 3116–3130. https://doi.org/10.1093/cercor/bht165

Anticevic, A., Haut, K., Murray, J. D., Repovs, G., Yang, G. J., Diehl, C., … Cannon, T.

D. (2015). Association of Thalamic Dysconnectivity and Conversion to Psychosis in Youth and Young Adults at Elevated Clinical Risk. *JAMA Psychiatry*, *72*(9), 882–891. https://doi.org/10.1001/jamapsychiatry.2015.0566.Association

Anticevic, A., Yang, G., Savic, A., Murray, J. D., Cole, M. W., Repovs, G., … Glahn, D. C. (2014). Mediodorsal and visual thalamic connectivity differ in schizophrenia and bipolar disorder with and without psychosis history. *Schizophrenia Bulletin*, *40*(6), 1227–1243. https://doi.org/10.1093/schbul/sbu100

Argyelan, M., Ikuta, T., Derosse, P., Braga, R. J., Burdick, K. E., John, M., … Szeszko, P. R. (2014). Resting-state fMRI connectivity impairment in schizophrenia and bipolar disorder. *Schizophrenia Bulletin*, *40*(1), 100–110. https://doi.org/10.1093/schbul/sbt092

Berretta, S. (2012). Extracellular matrix abnormalities in schizophrenia. *Neuropharmacology*, *62*(3), 1584–1597. https://doi.org/10.1016/j.neuropharm.2011.08.010

Berretta, S., Pantazopoulos, H., Markota, M., Brown, C., & Batzianouli, E. T. (2015). Losing the sugar coating: Potential impact of perineuronal net abnormalities on interneurons in schizophrenia. *Schizophrenia Research*, *167*(1–3), 18–27. https://doi.org/10.1016/j.schres.2014.12.040

Bleuler, E. (1911). *Dementia praecox oder die gruppe der schizophrenien*. Leipzig: Aschaffenburgs Handbuch, Deutike. (English edition: Bleuler, E. (1950). *Dementia praecox or the group of schizophrenias*. New York: International Universities Press).

Brown, C. G. (2014). *Extracellular matrix abnormalities in the amygdala of subjects*

with schizophrenia (Master's thesis). Retrieved from Hollis, Grossman Reserve PSY 143 2014 (Order No. 014248679).

Celio, M. R., Spreafico, R., De Biasi, S., & Vitellaro-Zuccarello, L. (1998). Perineuronal nets: Past and present. *Trends in Neurosciences*, *21*(12), 510–515. https://doi.org/10.1016/S0166-2236(98)01298-3

Chai, X. J., Whitfield-Gabrieli, S., Shinn, A. K., Gabrieli, J. D. E., Nieto Castañón, A., McCarthy, J. M., … Ongür, D. (2011). Abnormal medial prefrontal cortex resting-state connectivity in bipolar disorder and schizophrenia. *Neuropsychopharmacology*, *36*(10), 2009–17. https://doi.org/10.1038/npp.2011.88

Chong, H. Y., Teoh, S. L., Wu, D. B.-C., Kotirum, S., Chiou, C.-F., & Chaiyakunapruk, N. (2016). Global economic burden of schizophrenia: a systematic review. *Neuropsychiatric Disease and Treatment*, *12*, 357–73. https://doi.org/10.2147/NDT.S96649

Cullen, T. J., Walker, M. A., Parkinson, N., Craven, R., Crow, T. J., Esiri, M. M., & Harrison, P. J. (2003). A postmortem study of the mediodorsal nucleus of the thalamus in schizophrenia. *Schizophrenia Research*, *60*(2–3), 157–166. https://doi.org/10.1016/S0920-9964(02)00297-9

Danos, P., Baumann, B., Krämer, A., Bernstein, H. G., Stauch, R., Krell, D., … Bogerts, B. (2003). Volumes of association thalamic nuclei in schizophrenia: A postmortem study. *Schizophrenia Research*, *60*(2–3), 141–155. https://doi.org/10.1016/S0920-9964(02)00307-9

Danos, P., Schmidt, A., Baumann, B., Bernstein, H. G., Northoff, G., Stauch, R., …

Bogerts, B. (2005). Volume and neuron number of the mediodorsal thalamic nucleus in schizophrenia: A replication study. *Psychiatry Research - Neuroimaging*, *140*(3), 281–289. https://doi.org/10.1016/j.pscychresns.2005.09.005

Dorph-Petersen, K. A., & Lewis, D. A. (2016). Postmortem structural studies of the thalamus in schizophrenia. *Schizophrenia Research*, *180*, 28–35. https://doi.org/10.1016/j.schres.2016.08.007

Dorph-Petersen, K. A., Pierri, J. N., Sun, Z., Sampson, A. R., & Lewis, D. A. (2004). Stereological Analysis of the Mediodorsal Thalamic Nucleus in Schizophrenia: Volume, Neuron Number, and Cell Types. *Journal of Comparative Neurology*, *472*(4), 449–462. https://doi.org/10.1002/cne.20055

Grant, B. F., Stinson, F. S., Hasin, D. S., Dawson, D. a., Chou, S. P., Ruan, W. J., & Huang, B. (2005). Prevalence, Correlates, and Comorbidity of Bipolar I Disorder and Axis I and II Disorders: Results From the National Epidemiologic Survey on Alcohol and Related Conditions. *Journal of Clinical Psychiatry*, *66*(10), 1–11. https://doi.org/10.4088/JCP.v66n1001

Guidotti, A., Auta, J., Davis, J. M., Gerevini, V. D., Dwivedi, Y., Grayson, D. R., … Uzunov, D. (2000). Decrease in Reelin and Glutamic Acid Decarboxylase 67 (GAD 67) Expression in Schizophrenia and Bipolar Disorder. *Archives of General Psychiatry*, *57*(11), 1061–1069. https://doi.org/10.1001/archpsyc.57.11.1061

Harrison, P. J. (2016). Molecular neurobiological clues to the pathogenesis of bipolar

disorder. *Current Opinion in Neurobiology*, *36*, 1–6. https://doi.org/10.1016/j.conb.2015.07.002

Hayashi, N., Tatsumi, K., Okuda, H., Yoshikawa, M., Ishizaka, S., Miyata, S., Takanaka, M. & Wanaka, A. (2007). DACS, novel matrix structure composed of chondroitin sulfate proteoglycan in the brain. *Biochemical and Biophysical Research Communications*, *364*(2), 410–415. https://doi.org/10.1016/j.bbrc.2007.10.040

Horii-Hayashi, N., Tatsumi, K., Matsusue, Y., Okuda, H., Okuda, A., Hayashi, M., Yano, H., Tsuboi, A., Nishi, M., Yoshikawa, M., & Wanaka, A. (2010). Chondroitin sulfate demarcates astrocytic territories in the mammalian cerebral cortex. *Neuroscience Letters*, *483*(1), 67–72. https://doi.org/10.1016/j.neulet.2010.07.064

Jang, S. H., & Yeo, S. S. (2014). Thalamocortical connections between the mediodorsal nucleus of the thalamus and prefrontal cortex in the human brain: A diffusion tensor tractographic study. *Yonsei Medical Journal*, *55*(3), 709–714. https://doi.org/10.3349/ymj.2014.55.3.709

Javitt, D. C., & Freedman, R. (2015). Sensory processing dysfunction in the personal experience and neuronal machinery of schizophrenia. *American Journal of Psychiatry*, *172*(1), 17–31. https://doi.org/10.1176/appi.ajp.2014.13121691

Kahn, R. (2012). Brain Changes in Schizophrenia and Bipolar Disorder: Is There a Genetic Overlap? *Schizophrenia Research*, *136*(2012), S8. https://doi.org/10.1016/S0920-9964(12)70027-0

Lewis, D., & Lieberman, J. (2000). Catching up on schizophrenia: natural history and neurobiology. *Neuron*, *28*(2), 325–334. https://doi.org/S0896-6273(00)00111-2

Lewis, D. A., & Sweet, R. A. (2009). Schizophrenia from a neural circuitry perspective:

Advancing toward rational pharmacological therapies. *Journal of Clinical Investigation*, *119*(4), 706–716. https://doi.org/10.1172/JCI37335

Lindenmayer, J. P., Harvey, P. D., Khan, A., & Kirkpatrick, B. (2007). Schizophrenia: Measurements of Psychopathology. *Psychiatric Clinics of North America*, *30*(3), 339–363. https://doi.org/10.1016/j.psc.2007.04.005

MacDonald, A. W., & Schulz, S. C. (2009). What we know: Findings that every theory of Schizophrenia should explain. *Schizophrenia Bulletin*, *35*(3), 493–508. https://doi.org/10.1093/schbul/sbp017

Marcus, S. C., & Olfson, M. (2008). Outpatient antipsychotic treatment and inpatient costs of schizophrenia. *Schizophrenia Bulletin*, *34*(1), 173–180. https://doi.org/10.1093/schbul/sbm061

Marenco, S., Stein, J. L., Savostyanova, A. A., Sambataro, F., Tan, H.-Y., Goldman, A. L., … Weinberger, D. R. (2012). Investigation of Anatomical Thalamo-Cortical Connectivity and fMRI Activation in Schizophrenia. *Neuropsychopharmacology*, *37*(2), 499–507. https://doi.org/10.1038/npp.2011.215

Martinot, J. L., Hardy, P., Feline, A., Huret, J. D., Mazoyer, B., Attar-Levy, D., … Syrota, A. (1990). Left prefrontal glucose hypometabolism in the depressed state: A confirmation. *American Journal of Psychiatry*, *147*(10), 1313–1317. https://doi.org/10.1176/ajp.147.10.1313

Marvel, C. L., & Paradiso, S. (2004). Cognitive and neurological impairment in mood disorders. *Psychiatric Clinics of North America*, *27*(1), 1–17. https://doi.org/10.1016/S0193-953X(03)00106-0

Matuszko, G., Curreli, S., Kaushik, R., Becker, A., & Dityatev, A. (2017). Extracellular

matrix alterations in the ketamine model of schizophrenia. *Neuroscience*, *350*, 13–22. dx.doi.org/10.1016/j.neuroscience.2017.03.010

McGrath, J., Saha, S., Chant, D. & Welham, J. (2008). Schizophrenia: A concise overview of incidence, prevalence, and mortality. *Epidemiologic Reviews*, *30*(1), 67–76. https://doi.org/10.1093/epirev/mxn001

Merikangas, K. R., Jin, R., He, J. P., Kessler, R. C., Lee, S., Sampson, N. A., … Zarkov, Z. (2011). Prevalence and correlates of bipolar spectrum disorder in the world mental health survey initiative. *Arch.Gen.Psychiatry*, *68*, (1538–3636 (Electronic)), 241–251.

Meurs, J. (2016). The experimental design of postmortem studies: the effect size and statistical power. *Forensic Science, Medicine, and Pathology*, *12*(3), 343–349. https://doi.org/10.1007/s12024-016-9793-x

Miyata, S., Komatsu, Y., Yoshimura, Y., Taya, C., & Kitagawa, H. (2012). Persistent cortical plasticity by upregulation of chondroitin 6-sulfation. *Nature Neuroscience*, *15*(3), 414–422. https://doi.org/10.1038/nn.3023

Okuda, H., Tatsumi, K., Morita, S., Shibukawa, Y., Korekane, H., Horii-Hayashi, N., … Wanaka, A. (2014). Chondroitin sulfate proteoglycan tenascin-R regulates glutamate uptake by adult brain astrocytes. *Journal of Biological Chemistry*, *289*(5), 2620–2631. https://doi.org/10.1074/jbc.M113.504787

Ongür, D., Drevets, W. C., & Price, J. L. (1998). Glial reduction in the subgenual prefrontal cortex in mood disorders. *Proceedings of the National Academy of Sciences of the United States of America*, *95*(22), 13290–5. https://doi.org/10.1073/pnas.95.22.13290

Pakkenberg, B. (1990). Pronounced reduction of total neuron number in mediodorsal thalamic nucleus and nucleus accumbens in schizophrenics. *Archives of General Psychiatry*, *47*(11), 1023–8. https://doi.org/10.1001/archpsyc.1990.01810230039007

Pantazopoulos, H., Boyer-Boiteau, A., Holbrook, E. H., Jang, W., Hahn, C. G., Arnold, S. E., & Berretta, S. (2013). Proteoglycan abnormalities in olfactory epithelium tissue from subjects diagnosed with schizophrenia. *Schizophrenia Research*, *150*(2–3), 366–372. http://doi.org/10.1016/j.schres.2013.08.013

Pantazopoulos, H., Markota, M., Jaquet, F., Ghosh, D., Wallin, A., Santos, A., Caterson, B., & Berretta, S. (2015a). Aggrecan and chondroitin-6-sulfate abnormalities in schizophrenia and bipolar disorder: a postmortem study on the amygdala. *Translational Psychiatry*, *5*(1), e496. http://doi.org/10.1038/tp.2014.128

Pantazopoulos, H., Turiak, L., King, O., Zaia, J., & Berretta, S. (2015b). Chondroitin sulfate proteoglycan abnormalities are associated with altered thalamic axonal pathways in schizophrenia. *Neuropsychopharmocology*, *40*(1), S565-S566. http://doi.org/10.1038/tp.2014.128

Pantazopulos, H., Woo, T.-U. W., Lim, M., Lange, N., & Berretta, S. (2010). Extracellular matrix-glial abnormalities in the amygdala and entorhinal cortex of subjects diagnosed with schizophrenia. *Archives of General Psychiatry*, *67*(2), 155–166. https://doi.org/10.1001/archgenpsychiatry.2009.196

Peralta, V., & Cuesta, M. J. (2001). How many and which are the psychopathological

dimensions in schizophrenia? Issues influencing their ascertainment. *Schizophrenia Research*, *49*(3), 269–285. https://doi.org/10.1016/S0920-9964(00)00071-2

Pergola, G., Selvaggi, P., Trizio, S., Bertolino, A., & Blasi, G. (2015). The role of the thalamus in schizophrenia from a neuroimaging perspective. *Neuroscience and Biobehavioral Reviews*, *54*, 57–75. https://doi.org/10.1016/j.neubiorev.2015.01.013

Popken, G. J., Bunney Jr., W. E., Potkin, S. G., & Jones, E. G. (2000). Subnucleus-specific loss of neurons in medial thalamus of schizophrenics. *PNAS*, *97*(16), 9276–9280. https://doi.org/10.1073/pnas.150243397\r150243397

Rajkowska, G., Halaris, A., & Selemon, L. D. (2001). ORIGINAL ARTICLES Reductions in Neuronal and Glial Density Characterize the Dorsolateral Prefrontal Cortex in Bipolar Disorder. *Biological Psychiatry*, *49*(9), 741–752. https://doi.org/10.1016/S0006-3223(01)01080-0

Soares, J. C., & Mann, J. J. (1997). The functional neuroanatomy of mood disorders. *Journal of Psychiatric Research*, *31*(4), 393–432. https://doi.org/10.1016/S0022-3956(97)00016-2

Skåtun, K. C., Kaufmann, T., Brandt, C. L., Doan, N. T., Alnæs, D., Tønnesen, S., … Westlye, L. T. (2017). Thalamo-cortical functional connectivity in schizophrenia and bipolar disorder. *Brain Imaging and Behavior*. https://doi.org/10.1007/s11682-017-9714-y

Sykova, E. & Nicholson, C. (2008). Diffusion in brain extracellular space. *Physiology Review*, *88*, 1277–1340. https://doi.org/10.1152/physrev.00027.2007

Van der Werf, Y. D., Jolles, J., Witter, M. P., & Uylings, H. B. M. (2003). Contributions of thalamic nuclei to declarative memory functioning. *Cortex; a Journal Devoted to the Study of the Nervous System and Behavior*, *39*(4–5), 1047–62. https://doi.org/10.1016/S0010-9452(08)70877-3

Van Der Werf, Y. D., Weerts, J. G., Jolles, J., Witter, M. P., Lindeboom, J., & Scheltens, P. (1999). Neuropsychological correlates of a right unilateral lacunar thalamic infarction. *Journal of Neurology, Neurosurgery, and Psychiatry*, *66*(1), 36–42. https://doi.org/10.1136/jnnp.66.1.36

Welsh, R. C., Chen, A. C., & Taylor, S. F. (2010). Low-frequency BOLD fluctuations demonstrate altered thalamocortical connectivity in schizophrenia. *Schizophrenia Bulletin*, *36*(4), 713–722. https://doi.org/10.1093/schbul/sbn145

Woodward, N. D., Karbasforoushan, H., & Heckers, S. (2012). Thalamocortical dysconnectivity in schizophrenia. *American Journal of Psychiatry*, *169*(10), 1092–1099. https://doi.org/10.1176/appi.ajp.2012.12010056

Young, K. A., Manaye, K. F., Liang, C. L., Hicks, P. B., & German, D. C. (2000). Reduced number of mediodorsal and anterior thalamic neurons in schizophrenia. *Biological Psychiatry*, *47*(11), 944–953. https://doi.org/10.1016/S0006-3223(00)00826-X

Yu, K., Cheung, C., Leung, M., Li, Q., Chua, S., & McAlonan, G. (2010). Are Bipolar Disorder and Schizophrenia Neuroanatomically Distinct? An Anatomical Likelihood Meta-analysis. *Frontiers in Human Neuroscience*, *4*(189), 1–11. https://doi.org/10.3389/fnhum.2010.00189